

Decentralized real-time iterations for distributed NMPC

Gösta Stomberg, Alexander Engelmann, Moritz Diehl, and Timm Faulwasser

Abstract—This article presents a Real-Time Iteration (RTI) scheme for distributed Nonlinear Model Predictive Control (NMPC). The scheme transfers the well-known RTI approach, a key enabler for many industrial real-time NMPC implementations, to the setting of cooperative distributed control. At each sampling instant, one outer iteration of a bi-level decentralized Sequential Quadratic Programming (dSQP) method is applied to a centralized optimal control problem. This ensures that real-time requirements are met and it facilitates cooperation between subsystems. Combining novel dSQP convergence results with RTI stability guarantees, we prove local exponential stability under standard assumptions on the MPC design with and without terminal constraints. The proposed scheme only requires neighbor-to-neighbor communication and avoids a central coordinator. A numerical example with coupled inverted pendulums demonstrates the efficacy of the approach.

I. INTRODUCTION

Distributed control concerns the operation and control of cyber-physical systems, e.g., energy systems [1] or robot formations [2]. Coupling in systems of systems can occur in the dynamics, via constraints, or through a common objective. A key challenge for the design of optimization-based schemes for interconnected and cyber-physical systems is to reconcile cooperation with the computational burden, i.e., real-time feasibility is a must in applications. On the far end of the spectrum, decentralized control schemes do not allow for cooperation but also do not require communication between subsystems [3]. The opposite is centralized MPC, where the network of subsystems is considered as one, large-scale, dynamical system which is controlled by a single controller.

Model Predictive Control (MPC), also known as receding-horizon optimal control, has seen tremendous industrial success catalyzed by the development of numerical schemes tailored to the dynamics and to the problem formulation. Of particular importance for the implementation of centralized Nonlinear MPC (NMPC) are Real-Time Iteration (RTI) schemes [4–9]. Instead of solving the Optimal Control

Problem (OCP) to full accuracy in each control step, an RTI scheme applies only one or a few iterations of an optimization method.

On the other hand, Distributed MPC (DMPC) decomposes the numerical optimization among the subsystems [10, 11]. DMPC design proceeds mainly along two dimensions: (i) the OCP formulation and (ii) the implementation of an optimization algorithm with the desired degree of decomposition or decentralization.

With respect to (i), one may design either an individual OCP for each subsystem [12–14], or a centralized OCP for the whole cyber-physical system [15, 16]. Schemes with individual OCPs for the subsystems require few communication rounds per control step, enjoy small communication footprints, and allow for fast sampling rates [12–14]. However, they only allow for limited cooperation. Distributed approaches built upon centralized OCPs generally require multiple communication rounds per control step, but also allow for cooperation as the control tasks of all subsystems are encoded in the centralized OCP. We therefore refer to the latter approach as cooperative DMPC in this article.

With respect to (ii), numerous optimization algorithms have been proposed to solve centralized OCPs online [17–20]. A distinction can be made between distributed and decentralized optimization methods. Distributed optimization splits most computations between the subsystems and there exists a central entity which coordinates the subsystems [21]. Decentralized optimization only requires neighbor-to-neighbor communication without a coordinator [22].

Ultimately, cooperative DMPC aims to combine the high performance of centralized MPC with the favorable communication structure of decentralized optimization. Real-time requirements dictate that only a finite number of optimizer iterations can be executed in each control step, which limits performance and must be addressed in the stability analysis. While RTI schemes have been pivotal in bringing NMPC to industrial applications, distributed counterparts for similar results are not available. For linear systems, DMPC-specific OCP designs are presented in [15, 23] and stability under inexact optimization is analyzed in [24, 25]. For nonlinear systems, cooperative DMPC schemes with stability guarantees are presented in [16, 17]. In both articles, a centralized OCP with a terminal penalty is formulated such that the OCP value function serves as a candidate Lyapunov function for the closed-loop system. Stability is ensured in two different ways: Either a feasible-side convergent optimization method is employed and stability follows from standard arguments [17]. The drawback of this approach is

AE acknowledges support by the German Federal Ministry for Economic Affairs and Climate Action (BMWK) under agreement no. 03EI4043A (Redispatch3.0).

GS is with the Institute of Energy Systems, Energy Efficiency and Energy Economics, TU Dortmund University, 44227 Dortmund, Germany and with the Institute of Control Systems, Hamburg University of Technology, 21073 Hamburg, Germany (e-mail: goesta.stomberg@tu-dortmund.de).

AE and TF were with the Institute of Energy Systems, Energy Efficiency and Energy Economics, TU Dortmund University, 44227 Dortmund, Germany. AE is now with logarithmo GmbH & Co. KG, 44227 Dortmund, Germany (e-mail: alexander.engelmann@ieee.org). TF is now with the Institute of Control Systems, Hamburg University of Technology, 21073 Hamburg, Germany (e-mail: {alexander.engelmann, timm.faulwasser}@ieee.org).

MD is with the Department of Microsystems Engineering (IMTEK) and with the Department of Mathematics, University of Freiburg, 79104 Freiburg, Germany (e-mail: moritz.diehl@imtek.de).

that the optimization method requires a feasible initialization, which is difficult to implement in practice, and that each subsystem needs access to the dynamics of all subsystems in the network. The second option for guaranteeing stability is to solve the OCP with the Alternating Direction Method of Multipliers (ADMM) until a tailored ADMM stopping criterion is met [16]. This approach presumes that ADMM converges linearly, i.e., sufficiently fast, to the OCP minimizer. However, such ADMM convergence guarantees for problems with non-convex constraint sets are, to the best of the authors' knowledge, yet unavailable. Moreover, we note that the existing ADMM convergence guarantees for non-convex constraint sets [26, 27] so far do not allow for decentralized implementations.

Consequently, the existing stability guarantees of cooperative DMPC for coupled nonlinear systems either require feasible initialization and global model knowledge in *all* subsystems or they rely on rather strong assumptions on the achieved optimizer convergence. To overcome these limitations, we propose a novel decentralized RTI scheme for distributed NMPC. Our scheme builds on a bi-level decentralized Sequential Quadratic Programming (dSQP) scheme [28]. On the outer level, the method uses an inequality-constrained SQP scheme, which leads to partially separable convex Quadratic Programs (QPs) to be solved in each SQP step. On the inner level, these QPs are solved with ADMM which is guaranteed to converge and can be implemented in decentralized fashion, i.e., it does not require a central coordinator. Our previous conference paper [28] presents an earlier dSQP version including a stopping criterion for ADMM, but it does not consider real-time control applications and stability analysis. The idea of executing only few iterations of a tailored optimization method to enable distributed NMPC in real-time is also used in [19]. Therein, an augmented Lagrangian-based decomposition scheme is proposed for non-convex OCPs and suboptimality bounds for the optimizer solutions are derived, if changes in the system state between subsequent NMPC steps are small. While stability of the dynamical system is not formally discussed in [19], the approach shares commonalities to the scheme developed in this article and we later give a more detailed comparison in Remark 8 in Section V.

In the present paper, we explore the theoretical foundation of decentralized real-time iterations for DMPC via dSQP. The real-time feasibility of our approach has successfully been validated in experiments with mobile robots and on embedded hardware [29, 30] and the computational scalability for large-scale systems is investigated in [31]. Specifically, this article presents two contributions: First, we derive novel dSQP convergence guarantees when the number of inner iterations is fixed instead of relying on an inexact Newton type stopping criterion as in [28]. Second, we combine the linear convergence of dSQP with the RTI stability guarantees from [7] to derive the local exponential stability of the system-optimizer dynamics in closed loop. To the best of our knowledge, we are the first to study the system-optimizer convergence in DMPC and provide the respective ADMM

convergence guarantees.

The article is structured as follows: Section II states the control objective and presents the OCP. Section III recalls RTI stability for centralized NMPC. Section IV explains the bi-level dSQP scheme and derives new q-linear convergence guarantees when the number of inner iterations per outer iterations is fixed. Section V presents the stability of the distributed RTI scheme. Section VI analyzes numerical results for coupled inverted pendulums.

Notation: Given a matrix A and an integer j , $[A]_j$ denotes the j th row of A . For an index set \mathcal{A} , $[A]_{\mathcal{A}}$ denotes the matrix consisting of rows $[A]_j$ for all $j \in \mathcal{A}$. Likewise, $[a]_j$ is the j th component of vector a and $a_{\mathcal{A}}$ is the vector of components $[a]_j$ for all $j \in \mathcal{A}$. The concatenation of vectors x and y into a column vector is (x, y) . Given scalars a_1, \dots, a_n , $A = \text{diag}(a_1, \dots, a_n) \in \mathbb{R}^{n \times n}$ is the diagonal matrix where $[A]_{ii} = a_i$. Likewise, given matrices A_1, \dots, A_S , $C = \text{diag}(A_1, \dots, A_S)$ is a block diagonal matrix with block $[C]_{ii} = A_i$. The Euclidean norm of a vector $a \in \mathbb{R}^n$ is denoted by $\|a\| \doteq \sqrt{a^\top a}$. The spectral norm of a matrix $A \in \mathbb{R}^{n \times m}$ is denoted by $\|A\| \doteq \sigma_{\max}(A)$, the largest singular value of A . The closed ε neighborhood around a point $x^* \in \mathbb{R}^n$ is denoted as $\mathcal{B}(x^*, \varepsilon)$, i.e., $\mathcal{B}(x^*, \varepsilon) \doteq \{x \in \mathbb{R}^n \mid \|x - x^*\| \leq \varepsilon\}$. We denote the natural numbers by \mathbb{N} , the natural numbers extended by zero by $\mathbb{N}_0 \doteq \{0\} \cup \mathbb{N}$, the set of integers by \mathbb{I} , the set of integers in the range from 0 to N by $\mathbb{I}_{[0, N]}$, and the Minkowski sum of sets A and B as $A \oplus B$. Given $a \in \mathbb{R}$, $b = \lceil a \rceil$ is the nearest integer $b \geq a$.

II. PROBLEM STATEMENT

Consider a network $\mathcal{S} = \{1, \dots, S\}$ of dynamical systems connected by a graph $\mathcal{G} = (\mathcal{S}, \mathcal{E})$, where the edges $\mathcal{E} \subseteq \mathcal{S} \times \mathcal{S}$ couple neighboring subsystems. We define the set of subsystems which directly influence subsystem i as in-neighbors $\mathcal{N}_i^{\text{in}} \doteq \{j \in \mathcal{S} \setminus \{i\} \mid (j, i) \in \mathcal{E}\}$. Similarly, we collect the subsystems which are influenced by subsystem i in $\mathcal{N}_i^{\text{out}} \doteq \{j \in \mathcal{S} \setminus \{i\} \mid (i, j) \in \mathcal{E}\}$. We assume each subsystem $i \in \mathcal{S}$ can communicate with its neighbors $\mathcal{N}_i^{\text{in}}$ and $\mathcal{N}_i^{\text{out}}$.

We discuss distributed NMPC schemes for setpoint stabilization, where the subsystems cooperatively solve the OCP

$$\min_{\bar{x}, \bar{u}} \sum_{i \in \mathcal{S}} J_i(\bar{x}_i, \bar{u}_i, \bar{x}_{\mathcal{N}_i^{\text{in}}}) \quad (1a)$$

subject to for all $i \in \mathcal{S}$

$$\bar{x}_i(\tau+1) = f_i^\delta(\bar{x}_i(\tau), \bar{u}_i(\tau), \bar{x}_{\mathcal{N}_i^{\text{in}}}(\tau)), \quad \forall \tau \in \mathbb{I}_{[0, N-1]}, \quad (1b)$$

$$\bar{x}_i(0) = x_i(t), \quad (1c)$$

$$\bar{x}_i(\tau) \in \mathbb{X}_i, \forall \tau \in \mathbb{I}_{[0, N]}, \quad \bar{u}_i(\tau) \in \mathbb{U}_i, \forall \tau \in \mathbb{I}_{[0, N-1]}, \quad (1d)$$

$$(\bar{x}_i(\tau), \bar{x}_j(\tau)) \in \mathbb{X}_{ij}, \quad \forall j \in \mathcal{N}_i^{\text{in}}, \forall \tau \in \mathbb{I}_{[0, N]}, \quad (1e)$$

with objective functions

$$J_i(\cdot) \doteq \sum_{\tau=0}^{N-1} \ell_i(\bar{x}_i(\tau), \bar{u}_i(\tau), \bar{x}_{\mathcal{N}_i^{\text{in}}}(\tau)) + \beta V_{f,i}(\bar{x}_i(N)).$$

The state and input of subsystem i are denoted by $x_i \in \mathbb{R}^{n_{x_i}}$ and $u_i \in \mathbb{R}^{n_{u_i}}$, respectively. To distinguish closed-loop and

open-loop trajectories, we denote predicted states and inputs with a superscript $\bar{\cdot}$. The decision variables of OCP (1) are the predicted state trajectories \bar{x}_i and input trajectories \bar{u}_i over the horizon N . Define $n_i^{\text{in}} \doteq \sum_{j \in \mathcal{N}_i^{\text{in}}} n_{x_j}$. We stack the states of in-neighbors of subsystem i in alphabetical order in the vector $x_{\mathcal{N}_i^{\text{in}}} \in \mathbb{R}^{n_i^{\text{in}}}$. The objective (1a) consists of individual stage costs $\ell_i : \mathbb{R}^{n_{x_i}} \times \mathbb{R}^{n_{u_i}} \times \mathbb{R}^{n_i^{\text{in}}} \rightarrow \mathbb{R}$, terminal penalties $V_{f,i} : \mathbb{R}^{n_{x_i}} \rightarrow \mathbb{R}$, and a scaling factor $\beta \geq 1$. For all $i \in \mathcal{S}$, $f_i^\delta : \mathbb{R}^{n_{x_i}} \times \mathbb{R}^{n_{u_i}} \times \mathbb{R}^{n_i^{\text{in}}} \rightarrow \mathbb{R}^{n_{x_i}}$ denotes the discrete-time dynamics with control sampling interval $\delta > 0$. The states and inputs are constrained to the sets $\mathbb{X}_i \subseteq \mathbb{R}^{n_{x_i}}$, $\mathbb{U}_i \subseteq \mathbb{R}^{n_{u_i}}$. Each set $\mathbb{X}_{ij} \subseteq \mathbb{R}^{n_{x_i}} \times \mathbb{R}^{n_{x_j}}$ couples two neighbors $i, j \in \mathcal{S}$. We do not enforce additional terminal constraints to reduce the computational burden [32].

In our stability analysis, we view OCP (1) for the network \mathcal{S} as the following centralized OCP

$$V(x(t)) \doteq \min_{\bar{x}, \bar{u}} \sum_{\tau=0}^{N-1} \ell(\bar{x}(\tau), \bar{u}(\tau)) + \beta V_f(\bar{x}(N)) \quad (2a)$$

subject to

$$\bar{x}(\tau+1) = f^\delta(\bar{x}(\tau), \bar{u}(\tau)), \quad \forall \tau \in \mathbb{I}_{[0, N-1]}, \quad (2b)$$

$$\bar{x}(0) = x(t), \quad (2c)$$

$$\bar{x}(\tau) \in \mathbb{X}, \forall \tau \in \mathbb{I}_{[0, N]}, \bar{u}(\tau) \in \mathbb{U}, \forall \tau \in \mathbb{I}_{[0, N-1]}. \quad (2d)$$

The centralized system state and input are $x = (x_1, \dots, x_S) \in \mathbb{R}^{n_x}$ and $u = (u_1, \dots, u_S) \in \mathbb{R}^{n_u}$, respectively. The centralized discrete-time dynamics $f^\delta : \mathbb{R}^{n_x} \times \mathbb{R}^{n_u} \rightarrow \mathbb{R}^{n_x}$ are obtained by sampling the corresponding continuous-time dynamics $f^c : \mathbb{R}^{n_x} \times \mathbb{R}^{n_u} \rightarrow \mathbb{R}^{n_x}$ with piecewise constant input signals at $\delta > 0$. The partitioning of the centralized system into subsystems affects the performance of DMPC and is studied in [33].

The elements of OCP (2) are comprised of the components of (1). Considering the entire network as a single system of high state dimension serves as a conceptual means in the stability analysis and allows us to draw upon existing RTI stability guarantees. Notice that the numerical scheme to be proposed subsequently is decentralized, because we solve OCP (1) via dSQP [28].

III. CENTRALIZED REAL-TIME ITERATIONS

RTI schemes are designed to ensure the nominal closed-loop properties, if only few optimizer iterations are taken in each control step to compute a control input for system (2b). This section recalls stability guarantees that also hold when inequality constraints are present in the OCP [7].

To this end, we define the NMPC control law $\kappa_c : \mathbb{R}^{n_x} \rightarrow \mathbb{R}^{n_u}$ as the map from the initial state $x(t)$ in (2c) to the first part $\bar{u}^*(0)$ of the globally optimal input trajectory. We then make the following assumption on the value function $V : \mathbb{R}^{n_x} \rightarrow \mathbb{R}$, which can be met by appropriate OCP design, cf. [32]. OCP designs specific to DMPC are discussed in [12, 15, 23]. Define the level set $\mathbb{X}_{\bar{V}} \doteq \{x \in \mathbb{R}^{n_x} | V(x) \leq \bar{V}\}$ for a constant $\bar{V} > 0$.

Assumption 1 (Value function requirements [7]):

The value function $V : \mathbb{R}^{n_x} \rightarrow \mathbb{R}$ of OCP (2) is continuous

and there exist positive constants a_1, a_2, a_3, δ_0 , and \bar{V} such that, for all $x \in \mathbb{X}_{\bar{V}}$ and for all sampling intervals $\delta \leq \delta_0$,

$$a_1 \|x\|^2 \leq V(x) \leq a_2 \|x\|^2 \quad (3a)$$

$$V(f^\delta(x, \kappa_c(x))) - V(x) \leq -\delta \cdot a_3 \|x\|^2. \quad (3b)$$

Furthermore, there exists a constant $L_{V,x} > 0$ such that $|\sqrt{V(x)} - \sqrt{V(x')}| \leq L_{V,x} \|x - x'\|$ for all $x, x' \in \mathbb{X}_{\bar{V}}$. \square

Definition 1: Let $\bar{p} : \mathbb{R}^{n_x} \rightarrow \mathbb{R}^{n_p}$ be the map from the current state $x(t)$ in (2c) to the globally optimal primal-dual variables p^* of OCP (2). \square

Note that the control $\bar{u}^*(0)$ may be selected from the primal-dual variables p^* via a suitable matrix $M_{u,p} \in \mathbb{R}^{n_u} \times \mathbb{R}^{n_p}$ with $\|M_{u,p}\| = 1$, i.e., $\bar{u}^*(0) = M_{u,p} \bar{p}(x)$.

Assumption 2 (Lipschitz controller [7]): There exist positive constants \hat{r}_x and $L_{p,x}$ such that $\|\bar{p}(x') - \bar{p}(x)\| \leq L_{p,x} \|x' - x\|$ for all $x \in \mathbb{X}_{\bar{V}}$ and for all $x' \in \mathcal{B}(x, \hat{r}_x)$. Moreover, $\bar{p}(0) = 0$. \square

Note that $\bar{p}(0) = 0$ if the origin is an equilibrium of the system dynamics which minimizes ℓ and V_f , a common design choice in stabilizing NMPC. Put differently, this assumption does not hold for so-called economic NMPC schemes without further modification. The superscript \cdot^k denotes the iteration index of the optimization method which is used to solve OCP (2).

Assumption 3 (Q-linear optimizer convergence [7]):

There exist positive constants $\hat{r}_p > 0$ and $a_p < 1$ such that, for all $x \in \mathbb{X}_{\bar{V}}$ and for all $p^k \in \mathcal{B}(\bar{p}(x), \hat{r}_p)$, the optimization method initialized with p^k returns an iterate p^{k+1} satisfying

$$\|p^{k+1} - \bar{p}(x)\| \leq a_p \|p^k - \bar{p}(x)\|. \quad \square$$

Assumption 4 (Lipschitz system dynamics [7]): The centralized dynamics satisfy $f^c(0,0) = 0$. Consider r_p from Lemma 7 in Appendix I. There exist positive finite constants $\varrho, L_{f,x}^c$, and $L_{f,u}^c$ such that

$$\|f^c(x', u') - f^c(x, u)\| \leq L_{f,x}^c \|x' - x\| + L_{f,u}^c \|u' - u\|$$

for all $x', x \in \mathbb{X}_{\bar{V}} \oplus \mathcal{B}(0, \varrho)$ and for all $u' = M_{u,p} p'$, $u = M_{u,p} p$ with $p', p \in \mathcal{B}(\bar{p}(x), r_p)$. \square

At time t , the state $x(t)$ is sampled and the optimization method is initialized with the solution from the previous control step, i.e., $p^0(t) = p^{k_{\max}}(t-1)$, where $k_{\max} \in \mathbb{N}$ is the number of optimizer iterations per control step. Then, k_{\max} optimizer iterations are applied to the OCP, a primal-dual iterate $p^{k_{\max}}(t)$ is obtained, and the control input is selected. The control input is applied to the system and the primal-dual iterates are stored for the next time step. The optimization method and the system together form the system-optimizer dynamics [7]

$$\begin{bmatrix} x(t+1) \\ p^{k_{\max}}(t+1) \end{bmatrix} = \begin{bmatrix} f^\delta(x(t), M_{u,p} p^{k_{\max}}(t)) \\ \Phi(x(t), p^{k_{\max}}(t)) \end{bmatrix}, \quad (4)$$

where $\Phi : \mathbb{R}^{n_x} \times \mathbb{R}^{n_p} \rightarrow \mathbb{R}^{n_p}$ maps the OCP initial state $x(t)$ and approximate solution $p^{k_{\max}}(t)$ to the approximate solution $p^{k_{\max}}(t+1)$ at the next time step.

Lemma 1 (Centralized RTI stability [7]): Suppose that Assumptions 1–4 hold and consider the sufficient sampling

interval $\bar{\delta}$ and optimizer initialization radius \tilde{r}_p defined in (29) in Appendix I. If $\delta \leq \bar{\delta}$, $x(0) \in \mathbb{X}_{\bar{V}}$, and $p^0(0) \in \mathcal{B}(\bar{p}(x(0)), \tilde{r}_p)$, then the origin is an exponentially stable equilibrium for the closed-loop system-optimizer dynamics (4). \square

Remark 1 (Relation to [7]): Lemma 1 is a specialized variant of [7, Thm. 25] in three aspects: First, we only consider quadratic bounds on the Lyapunov function. Second, we define the map \bar{p} from the current state to the primal-dual variables, because of the dSQP convergence presented in the next section. Third, we allow for $k_{\max} \geq 1$ optimizer iterations. In contrast, [7, Thm. 25] considers more general Lyapunov functions, allows for any Lipschitz continuous map $\bar{p} : \mathbb{R}^{n_x} \rightarrow \mathbb{R}^{n_p}$ such that $\bar{u}^*(0) = M_{u,p}\bar{p}(x)$, and considers $k_{\max} = 1$. Note that the extension to $k_{\max} > 1$ is straight forward because of the q-linear optimizer convergence in Assumption 3. \square

IV. DECENTRALIZED SEQUENTIAL QUADRATIC PROGRAMMING

The crucial requirement on the optimization method to guarantee closed-loop stability via Lemma 1 is local q-linear convergence. Hence we now recall dSQP from [28] and derive the required convergence property.

By introducing state trajectory copies for neighboring subsystems, OCP (1) can be written as a partially separable Nonlinear Program (NLP) [16, 18]

$$\min_z \sum_{i \in \mathcal{S}} f_i(z_i) \quad (5a)$$

$$\text{subject to } g_i(z_i) = 0 \mid \nu_i \quad \forall i \in \mathcal{S}, \quad (5b)$$

$$h_i(z_i) \leq 0 \mid \mu_i \quad \forall i \in \mathcal{S}, \quad (5c)$$

$$\sum_{i \in \mathcal{S}} E_i z_i = c \mid \lambda. \quad (5d)$$

The decision variables $z_i \in \mathbb{R}^{n_i}$ of subsystem i include the predicted trajectories \bar{x}_i and \bar{u}_i over the horizon as well as copies of the predicted state trajectories of neighboring subsystems. Example 1 in Appendix II illustrates the reformulation of OCP (2) as a partially separable NLP like (5). The functions $f_i : \mathbb{R}^{n_i} \rightarrow \mathbb{R}$, $g_i : \mathbb{R}^{n_i} \rightarrow \mathbb{R}^{n_{g_i}}$, and $h_i : \mathbb{R}^{n_i} \rightarrow \mathbb{R}^{n_{h_i}}$ are composed of the objective functions, equality constraints, and inequality constraints in OCP (1), respectively.

Assumption 5 (Differentiability of the NLP functions):

The functions f_i , g_i , and h_i are three times continuously differentiable for all $i \in \mathcal{S}$. \square

The sparse matrices $E_i \in \mathbb{R}^{n_c \times n_i}$ couple the subsystems by matching original and copied variables of state trajectories. Thus, the sparsity pattern of the matrices E_i arises from the coupling graph \mathcal{G} . Specifically, (i, j) or $(j, i) \in \mathcal{E}$ if and only if there exists an index $o \in \{1, \dots, n_c\}$ such that $[E_i]_o \neq 0$ and $[E_j]_o \neq 0$.

The notation in NLP (5) highlights that $\nu_i \in \mathbb{R}^{n_{g_i}}$, $\mu_i \in \mathbb{R}^{n_{h_i}}$, and $\lambda \in \mathbb{R}^{n_c}$ are Lagrange multipliers associated with the respective constraints. The centralized variables are $z \doteq (z_1, \dots, z_S) \in \mathbb{R}^n$, $\nu \doteq (\nu_1, \dots, \nu_S) \in \mathbb{R}^{n_g}$,

and $\mu \doteq (\mu_1, \dots, \mu_S) \in \mathbb{R}^{n_h}$. Likewise, we denote the centralized constraints as $g(z) \doteq (g_1(z_1), \dots, g_S(z_S))$ and $h(z) \doteq (h_1(z_1), \dots, h_S(z_S))$. Throughout this section, we denote the globally optimal Karush-Kuhn-Tucker (KKT) point of NLP (5) with initial condition $x \in \mathbb{X}_{\bar{V}}$ as $p^* = (z^*, \nu^*, \mu^*, \lambda^*) \doteq \bar{p}(x)$, cf. Definition 1. That is, the notation p^* drops the explicit dependence on x for simplicity and we keep in mind that the KKT point depends on the initial state.

We define the Lagrangian to NLP (5) as

$$L(z, \nu, \mu, \lambda) = \sum_{i \in \mathcal{S}} L_i(z_i, \nu_i, \mu_i, \lambda) - \lambda^\top c,$$

where $L_i \doteq \sum_{i \in \mathcal{S}} (f_i(z_i) + \nu_i^\top g_i(z_i) + \mu_i^\top h_i(z_i) + \lambda^\top E_i z_i)$.

The bi-level dSQP method from [28] combines an SQP scheme on the outer level with ADMM on the inner level. We index outer iterations by \cdot^k and inner iterations by \cdot^l . Starting from a primal-dual point $p^k = (z^k, \nu^k, \mu^k, \lambda^k)$, the method proceeds as follows. In each SQP iteration, we first construct a quadratic approximation of NLP (5)

$$\min_z \sum_{i \in \mathcal{S}} f_i^{\text{QP},k}(z_i) \quad (6a)$$

$$\text{subject to } g_i^k + \nabla g_i^{k\top}(z_i - z_i^k) = 0 \mid \nu_i \quad \forall i \in \mathcal{S}, \quad (6b)$$

$$h_i^k + \nabla h_i^{k\top}(z_i - z_i^k) \leq 0 \mid \mu_i \quad \forall i \in \mathcal{S}, \quad (6c)$$

$$\sum_{i \in \mathcal{S}} E_i z_i = c \mid \lambda, \quad (6d)$$

where, $f_i^{\text{QP},k} \doteq (z_i - z_i^k)^\top H_i^k (z_i - z_i^k)/2 + \nabla f_i^{k\top}(z_i - z_i^k)$, and where, for all $i \in \mathcal{S}$, $H_i^k \approx \nabla_{z_i z_i}^2 L_i(z_i^k, \nu_i^k, \mu_i^k)$ is positive definite on the space spanned by (6b). The symbols g_i^k and ∇g_i^k in QP (6) are shorthands for $g_i(z_i^k)$ and $\nabla g_i(z_i^k)$, respectively. The same holds for functions f_i and h_i . We denote the unique centralized primal dual-solution to QP (6) as $p_{\text{QP}}^{k,*} = (z_{\text{QP}}^{k,*}, \nu_{\text{QP}}^{k,*}, \mu_{\text{QP}}^{k,*}, \lambda_{\text{QP}}^{k,*})$ and the centralized Hessian as $H^k \doteq \text{diag}(H_1^k, \dots, H_S^k)$.

Then, we apply a fixed number l_{\max} of ADMM iterations to QP (6). To this end, we introduce the decision variable $y \in \mathbb{R}^n$ and reformulate QP (6) in two-block form as

$$\min_{\substack{y_1 \in \mathbb{Z}_1^k, \dots, y_S \in \mathbb{Z}_S^k \\ z \in \mathbb{E}}} \sum_{i \in \mathcal{S}} f_i^{\text{QP},k}(y_i) \quad (7a)$$

$$\text{subject to } y_i - z_i = 0 \mid \gamma_i \quad \forall i \in \mathcal{S}. \quad (7b)$$

The subsystem constraint sets are defined as

$$\mathbb{Z}_i^k \doteq \left\{ y_i \in \mathbb{R}^{n_i} \mid \begin{cases} g_i^k + \nabla g_i^{k\top}(y_i - z_i^k) = 0 \\ h_i^k + \nabla h_i^{k\top}(y_i - z_i^k) \leq 0 \end{cases} \right\},$$

the consensus constraint set is

$$\mathbb{E} \doteq \left\{ z \in \mathbb{R}^n \mid \sum_{i \in \mathcal{S}} E_i z_i = c \right\},$$

and $\gamma_i \in \mathbb{R}^{n_i}$ is the Lagrange multiplier to constraint (7b). We denote the centralized multiplier as $\gamma \doteq (\gamma_1, \dots, \gamma_S)$ and define the augmented Lagrangian for QP (7) as

$$L_\rho^k(y, z, \gamma) = \sum_{i \in \mathcal{S}} L_{\rho,i}^k(y_i, z_i, \gamma_i),$$

in control only allow for a small number l_{\max} of ADMM iterations per SQP iteration in Algorithm 2. Hence, we now consider an inexact SQP scheme where p^{k+1} only approximates the primal-dual solution $p_{\text{QP}}^{k,*}$ of QP (6).

Lemma 3 (Inexact SQP convergence): Suppose Assumption 5 holds and let p^* denote a KKT point which satisfies Assumption 6. Form QP (6) at a primal-dual point $p^k = (z^k, \nu^k, \mu^k, \lambda^k)$ using the exact Hessian $H^k = \nabla_{zz}^2 L(z^k, \nu^k, \mu^k)$. Consider an inexact SQP scheme, whose iterates $\{p^k\}$, for all $k \in \mathbb{N}_0$ and for some $a < 1$, satisfy

$$\|p^{k+1} - p_{\text{QP}}^{k,*}\| \leq a \|p^k - p_{\text{QP}}^{k,*}\|. \quad (9)$$

Furthermore, let $\bar{a}_p \in (a, 1)$. Then, there exists $\varepsilon_2 > 0$ such that the following holds. If $p^0 \in \mathcal{B}(p^*, \varepsilon_2)$, then the sequence $\{p^k\}$ generated by the inexact SQP scheme converges q-linearly to p^* , $\|p^{k+1} - p^*\| \leq \bar{a}_p \|p^k - p^*\|$ for all $k \in \mathbb{N}_0$. \square

Proof: By Lemma 2, the convergence radius of the exact SQP scheme is thus given by $\varepsilon_1 > 0$. Let $\varepsilon_2 \leq \varepsilon_1$. From Lemma 2 we have for all $k \in \mathbb{N}_0$ that QP (6) is feasible and

$$\|p_{\text{QP}}^{k,*} - p^*\| \leq C \|p^k - p^*\|^2. \quad (10)$$

Combining (9) and (10) yields

$$\begin{aligned} \|p^{k+1} - p^*\| &\leq \|p^{k+1} - p_{\text{QP}}^{k,*}\| + \|p_{\text{QP}}^{k,*} - p^*\| \\ &\leq a \|p^k - p_{\text{QP}}^{k,*}\| + \|p_{\text{QP}}^{k,*} - p^*\| \\ &\leq a \|p^k - p^*\| + (1+a) \|p_{\text{QP}}^{k,*} - p^*\| \\ &\leq a \|p^k - p^*\| + (1+a)C \|p^k - p^*\|^2. \end{aligned}$$

Choosing $\|p^0 - p^*\| < (\bar{a}_p - a)/((1+a)C)$ with $a < \bar{a}_p < 1$, we obtain for all $k \in \mathbb{N}_0$

$$\|p^{k+1} - p^*\| \leq \bar{a}_p \|p^k - p^*\|.$$

Hence, if $p^0 \in \mathcal{B}(p^*, \varepsilon_2)$ and if $\varepsilon_2 \leq \min(\varepsilon_1, (\bar{a}_p - a)/((1+a)C))$, then the sequence $\{p^k\}$ converges q-linearly to p^* . \blacksquare

Lemma 3 guarantees local SQP convergence, if the inexact QP solutions satisfy inequality (9) as in [38, Lem. 3.1.10]. As we show next, the solutions produced by ADMM meet this requirement.

B. Inner Convergence

We next derive a sufficiently large number of ADMM iterations l_{\max} that guarantees inexact SQP convergence via (9). To this end, we first express l_{\max} based on constants associated with the ADMM convergence for convex QPs. Subsequently, we quantify the constants to compute l_{\max} inside a local convergence region where the active set stays constant. Define $c_1 \doteq \max\{1, \|E^\top\|/\rho\}$, the ADMM averaging matrix $M_{\text{avg}} \doteq I - E^\top (EE^\top)^{-1} E$,

$$D_1 \doteq \begin{bmatrix} M_{\text{avg}} \\ (EE^\top)^{-1} E \rho \end{bmatrix} \begin{bmatrix} I & I \end{bmatrix},$$

and $d_1 \doteq \|D_1\|$. Furthermore, given a constant d_2 , define $c_2 \doteq d_1 + d_1 d_2 + d_2$.

Lemma 4 (ADMM convergence): Suppose Assumption 5 holds and let p^* denote a KKT point which satisfies Assumption 6. Form QP (6) at a primal-dual point $p^k = (z^k, \nu^k, \mu^k, \lambda^k)$ using the exact Hessian $H^k = \nabla_{zz}^2 L(z^k, \nu^k, \mu^k)$. Initialize Algorithm 1 with z_i^k and $E_i^\top \lambda^k$ for all $i \in \mathcal{S}$. Then, there exist an ADMM contraction factor $0 < a_w < 1$ and constants $d_2, \varepsilon > 0$ such that the following holds for all $0 < a < 1$. If $p^k \in \mathcal{B}(p^*, \varepsilon)$ and if

$$l_{\max} \geq 1 + \max \left\{ 0, \left\lceil \log_{a_w} \left(\frac{a}{c_1 c_2} \right) \right\rceil \right\}, \quad (11)$$

then the iterates $p^{l_{\max}} = (z^{l_{\max}}, \nu^{l_{\max}}, \mu^{l_{\max}}, \lambda^{l_{\max}})$ returned by Algorithm 1 satisfy

$$\|p^{l_{\max}} - p_{\text{QP}}^{k,*}\| \leq a \|p^k - p_{\text{QP}}^{k,*}\|.$$

Furthermore, the active set stays constant, i.e., for all $i \in \mathcal{S}$

$$[h_i^k + \nabla h_i^{k\top} (y_i^l - z_i^k)]_{A_i} = 0 \quad \forall l \in \mathbb{N}, \quad \square$$

Proof: The proof proceeds in five steps. First, (a), we show that $p_{\text{QP}}^{k,*}$ is regular, if $p^k \approx p^*$. Then, (b), ADMM converges q-linearly in the vector $w \doteq (z, \gamma/\rho)$, because QP (6) is strictly convex over the constraint set. Then, (c), we apply the BST to the subsystem QPs and obtain that the active set is constant. Then, (d), we bound the error of the ADMM averaging step. Finally, (e), we derive the iteration bound (11).

(a) Let $\varepsilon \leq \varepsilon_1$. By the regularity of the KKT point p^* , (Assumption 6), the solution to QP (6) formed at p^* is also regular, i.e., if $p^k = p^*$, then the QP solution $p_{\text{QP}}^{k,*}$ satisfies strict complementarity, LICQ, and the stronger SOSC

$$y^\top H^k y > 0 \text{ for all } y \neq 0 \text{ with } \nabla g(z^k)^\top y = 0. \quad (12)$$

We can regard QP (6) formed at $p^k \approx p^*$ as a perturbed version of the QP formed at p^* . Because of Assumption 5, we can apply the BST [39, Thm. 3.2.2] to QP (6) and thus there exists $\varepsilon > 0$ such that the solution $p_{\text{QP}}^{k,*}$ to the perturbed QP (6) is regular for all $p^k \in \mathcal{B}(p^*, \varepsilon)$. The stronger SOSC condition (12) also holds if $p^k \in \mathcal{B}(p^*, \varepsilon)$, which follows by adjusting the proof of the BST to the fact that Assumption 6 (ii) is slightly stronger than SOSC [39, Lem. 3.2.1].

(b) From (a) we have that LICQ holds at $p_{\text{QP}}^{k,*}$ for all $p^k \in \mathcal{B}(p^*, \varepsilon)$. Thus, the Jacobian $\nabla g_i^{k\top} \in \mathbb{R}^{n_{g_i} \times n_i}$ has full row rank for all $i \in \mathcal{S}$. Recall that for any $A \in \mathbb{R}^{m \times n}$, by the fundamental theorem of linear algebra, the null space of A and the range space of A^\top together form \mathbb{R}^n [40, p. 603]. For all $i \in \mathcal{S}$, we can thus decompose any point $y_i \in \mathbb{R}^{n_i}$ via the null space method [40, Ch. 16] as

$$y_i = Z_i^k v_i + \nabla g_i^k w_i$$

with vectors $v_i \in \mathbb{R}^{n_i - n_{g_i}}$ and $w_i \in \mathbb{R}^{n_{g_i}}$, and a null space basis $Z_i^k \in \mathbb{R}^{n_i \times (n_i - n_{g_i})}$ of $\nabla g_i^{k\top}$. That is, $\nabla g_i^{k\top} Z_i^k = 0$. If $y_i \in \mathbb{Z}_i^k$, then w_i is uniquely determined by the equality constraints (6b): $w_i = -(\nabla g_i^{k\top} \nabla g_i^k)^{-1} g_i^k$, which follows from the full row rank of $\nabla g_i^{k\top}$. Moreover, the stronger SOSC condition (12) implies that the reduced Hessian $\bar{H}_i^k \doteq Z_i^{k\top} H_i^k Z_i^k$ is positive definite for all $i \in \mathcal{S}$. Because w_i

is fixed for $y_i \in \mathbb{Z}_i^k$ and because \bar{H}_i^k is positive definite, the objective $f_i^{\text{QP},k}$ is strictly convex over the set \mathbb{Z}_i^k for all $i \in \mathcal{S}$. Thus, $p_{\text{QP}}^{k,*}$ is the only KKT point of QP (6). Furthermore, the sets \mathbb{Z}^k and \mathbb{E} are closed and convex polyhedra, and they are feasible because $\varepsilon \leq \varepsilon_1$. Therefore, and because $f_i^{\text{QP},k}$ are strictly convex over \mathbb{Z}_i^k for all $i \in \mathcal{S}$, ADMM converges q-linearly in w and, for all $p^k \in \mathcal{B}(p^*, \varepsilon)$,

$$\|w^{l+1} - w_{\text{QP}}^{k,*}\| \leq a_w \|w^l - w_{\text{QP}}^{k,*}\| \quad (13)$$

for some $a_w < 1$ and for all $l \in \mathbb{N}_0$ [41, Thm. 14].

(c) The first ADMM step (8a) solves a parametric QP, whose objective affinely depends on $(\rho z^l, \gamma^l) = \rho w^l$. The error $w^l - w_{\text{QP}}^{k,*}$ thus perturbs the QP in (8a). If (8a) is parameterized with $w_{\text{QP}}^{k,*}$, then the step (8a) returns $y_{\text{QP}}^{k,*}$, $\nu_{\text{QP}}^{k,*}$, and $\mu_{\text{QP}}^{k,*}$. Thus, by the same arguments as in (a), the QP in step (8a) formed at $w_{\text{QP}}^{k,*}$ satisfies strict complementarity, LICQ, and the stronger SOSC condition (12) for all $p^k \in \mathcal{B}(p^*, \varepsilon)$. We can therefore apply the BST to the perturbed subsystem QP in step (8a). Thus, there exists $\varepsilon_3 > 0$ such that the map from $w^l - w_{\text{QP}}^{k,*}$ to $(y^{l+1}, \nu^{l+1}, \mu^{l+1})$ is continuously differentiable and the active set is constant for all $w^l \in \mathcal{B}(w_{\text{QP}}^{k,*}, \varepsilon_3)$. That is, if $w^l \in \mathcal{B}(w_{\text{QP}}^{k,*}, \varepsilon_3)$, then

$$\begin{aligned} [h_i^k + \nabla h_i^{k\top} (y_i^{l+1} - z_i^k)]_{\mathcal{A}_i} &= 0 \quad \forall i \in \mathcal{S} \\ [\mu_i^{l+1}]_{\mathcal{I}_i} &= 0 \quad \forall i \in \mathcal{S}. \end{aligned}$$

Since local continuous differentiability implies local Lipschitz continuity, there exists a constant $d_2 < \infty$ such that, for all $w^l \in \mathcal{B}(w_{\text{QP}}^{k,*}, \varepsilon_3)$ and for all $p^k \in \mathcal{B}(p^*, \varepsilon)$,

$$\left\| \begin{bmatrix} y^{l+1} \\ \nu^{l+1} \\ \mu^{l+1} \end{bmatrix} - \begin{bmatrix} y_{\text{QP}}^{k,*} \\ \nu_{\text{QP}}^{k,*} \\ \mu_{\text{QP}}^{k,*} \end{bmatrix} \right\| \leq d_2 \|w^l - w_{\text{QP}}^{k,*}\|. \quad (14)$$

Because of the q-linear ADMM convergence (13), there exists $\varepsilon > 0$ such that $w^l \in \mathcal{B}(w_{\text{QP}}^{k,*}, \varepsilon_3)$ for all $l \in \mathbb{N}_0$, if $p^k \in \mathcal{B}(p^*, \varepsilon)$.

(d) Define $\Delta y^l \doteq y^l - y_{\text{QP}}^{k,*}$, $\Delta z^l \doteq z^l - z_{\text{QP}}^{k,*}$, $\Delta \nu^l \doteq \nu^l - \nu_{\text{QP}}^{k,*}$, $\Delta \mu^l \doteq \mu^l - \mu_{\text{QP}}^{k,*}$, $\Delta \lambda^l \doteq \lambda^l - \lambda_{\text{QP}}^{k,*}$, and $\Delta \gamma^l \doteq \gamma^l - \gamma_{\text{QP}}^{k,*}$. The KKT conditions of the coordination QP in (8b) yield

$$\begin{aligned} z^{l+1} &= M_{\text{avg}} (y^{l+1} + \gamma^l / \rho) + E^\top (EE^\top)^{-1} c, \\ \lambda^{l+1} &= (EE^\top)^{-1} E \rho (y^{l+1} + \gamma^l / \rho) - (EE^\top)^{-1} \rho c \end{aligned}$$

for all $l \in \mathbb{N}_0$. Likewise,

$$\begin{aligned} z_{\text{QP}}^{k,*} &= M_{\text{avg}} (y_{\text{QP}}^{k,*} + \gamma_{\text{QP}}^{k,*} / \rho) + E^\top (EE^\top)^{-1} c, \\ \lambda_{\text{QP}}^{k,*} &= (EE^\top)^{-1} E \rho (y_{\text{QP}}^{k,*} + \gamma_{\text{QP}}^{k,*} / \rho) - (EE^\top)^{-1} \rho c \end{aligned}$$

and hence

$$\begin{bmatrix} \Delta z^{l+1} \\ \Delta \lambda^{l+1} \end{bmatrix} = \underbrace{\begin{bmatrix} M_{\text{avg}} \\ (EE^\top)^{-1} E \rho \end{bmatrix}}_{D_1} \begin{bmatrix} I & I \end{bmatrix} \begin{bmatrix} \Delta y^{l+1} \\ \Delta \gamma^{l+1} / \rho \end{bmatrix}. \quad (15)$$

Since $d_1 = \|D_1\|$, we obtain, for all $l \in \mathbb{N}_0$,

$$\left\| \begin{bmatrix} \Delta z^{l+1} \\ \Delta \lambda^{l+1} \end{bmatrix} \right\| \leq d_1 \left\| \begin{bmatrix} \Delta y^{l+1} \\ \Delta \gamma^{l+1} / \rho \end{bmatrix} \right\|. \quad (16)$$

(e) Combining the continuity properties (14) and (16) yields, for all $p^k \in \mathcal{B}(p^*, \varepsilon)$ and for all $l \in \mathbb{N}_0$,

$$\begin{aligned} \|p^{l+1} - p_{\text{QP}}^{k,*}\| &= \left\| \begin{bmatrix} \Delta z^{l+1} \\ \Delta \nu^{l+1} \\ \Delta \mu^{l+1} \\ \Delta \lambda^{l+1} \end{bmatrix} \right\| \\ &\leq \left\| \begin{bmatrix} \Delta \nu^{l+1} \\ \Delta \mu^{l+1} \end{bmatrix} \right\| + \left\| \begin{bmatrix} \Delta z^{l+1} \\ \Delta \lambda^{l+1} \end{bmatrix} \right\| \\ &\leq d_2 \|w^l - w_{\text{QP}}^{k,*}\| + d_1 \left\| \begin{bmatrix} \Delta y^{l+1} \\ \Delta \gamma^{l+1} / \rho \end{bmatrix} \right\| \\ &\leq d_2 \|w^l - w_{\text{QP}}^{k,*}\| + d_1 \|\Delta y^{l+1}\| + d_1 \|\Delta \gamma^{l+1} / \rho\| \\ &\leq \underbrace{(d_1 + d_1 d_2 + d_2)}_{=c_2} \|w^l - w_{\text{QP}}^{k,*}\|. \quad (17) \end{aligned}$$

The KKT system of QP (7) implies $\gamma_{\text{QP}}^{k,*} = E^\top \lambda_{\text{QP}}^{k,*}$ and the KKT system of the coupling QP in Step (8b) yields $\rho(z^{l+1} - y^{l+1}) - \gamma^{l+1} + E^\top \lambda^{l+1} = 0$. Inserting the last equation into the ADMM dual update (8c) gives $\gamma^{l+1} = E^\top \lambda^{l+1}$ for all $l \in \mathbb{N}_0$. Combining this with the definitions of w and p and with the initialization $\gamma_i^0 = E_i^\top \lambda^0$ for $k = 0$ yields, for all $l \in \mathbb{N}_0$,

$$w^l - w_{\text{QP}}^{k,*} = \begin{bmatrix} I & 0 & 0 & 0 \\ 0 & 0 & 0 & E^\top / \rho \end{bmatrix} (p^l - p_{\text{QP}}^{k,*})$$

and hence

$$\|w^l - w_{\text{QP}}^{k,*}\| \leq \underbrace{\left\| \begin{bmatrix} I & 0 & 0 & 0 \\ 0 & 0 & 0 & E^\top / \rho \end{bmatrix} \right\|}_{c_1} \|p^l - p_{\text{QP}}^{k,*}\|. \quad (18)$$

Combining the q-linear convergence (13) with the Lipschitz bounds (17)–(18) yields, for all $p^k \in \mathcal{B}(p^*, \varepsilon)$,

$$\begin{aligned} \|p^{k+1} - p_{\text{QP}}^{k,*}\| &= \|p^{l_{\text{max}}} - p_{\text{QP}}^{k,*}\| \\ &\leq c_2 \|w^{l_{\text{max}}-1} - w_{\text{QP}}^{k,*}\| \\ &\leq c_2 (a_w)^{l_{\text{max}}-1} \|w^k - w_{\text{QP}}^{k,*}\| \\ &\leq \underbrace{c_1 c_2 (a_w)^{l_{\text{max}}-1}}_{\doteq a} \|p^k - p_{\text{QP}}^{k,*}\|. \end{aligned}$$

Rearranging $a = c_1 c_2 (a_w)^{l_{\text{max}}-1}$ yields

$$l_{\text{max}} = 1 + \log_{a_w} \left(\frac{a}{c_1 c_2} \right).$$

The algorithm is only well-defined if $l_{\text{max}} \geq 1$ and thus we obtain the inner iteration bound (11). ■

The bound (11) depends on the ADMM contraction factor a_w in (13), the constant d_2 in the subsystem QP error (14), and a . The constants a_w , c_1 , and c_2 depend on the penalty parameter ρ and can thus be tuned for a given problem. The design parameter $a \in (0, 1)$ controls the accuracy to which ADMM solves QP (6): choosing a small increases l_{max} in (11), but also allows for a larger sampling interval $\bar{\delta}$ in the stability guarantee.

The q-linear convergence (13) of ADMM is global, i.e., it holds for any $w^l \in \mathbb{R}^{2n}$. To the best of our knowledge, there does not yet exist a quantification of the contraction

factor a_w for the global ADMM convergence that would be applicable here. However, we can quantify a_w and d_2 for $w^l \approx w_{\text{QP}}^{k,*}$ inside the area of constant active set as follows.

Denote the centralized active and inactive sets as $\mathcal{A} \doteq \{j \in \{1, \dots, n_h\} \mid [h(z^*)]_j = 0\}$ and $\mathcal{I} \doteq \{j \in \{1, \dots, n_h\} \mid [h(z^*)]_j < 0\}$, respectively. Furthermore, define the shorthands $h_{\mathcal{A}}^k \doteq [h(z^k)]_{\mathcal{A}}$, $\nabla h_{\mathcal{A}}^{k\top} \doteq [\nabla h(z^k)]_{\mathcal{A}}^\top$, $\mu_{\mathcal{A}} \doteq [\mu]_{\mathcal{A}}$, and $\mu_{\mathcal{I}} \doteq [\mu]_{\mathcal{I}}$. The centralized KKT matrix of the subsystem QPs in Step (8a) is regular for all $p^k \in \mathcal{B}(p^*, \varepsilon)$ with ε from Lemma 4 and reads

$$K^k \doteq \begin{bmatrix} H^k + \rho I & \nabla g^k & \nabla h_{\mathcal{A}}^k \\ \nabla g^{k\top} & 0 & 0 \\ \nabla h_{\mathcal{A}}^{k\top} & 0 & 0 \end{bmatrix}.$$

For all $p^k \in \mathcal{B}(p^*, \varepsilon)$, we define the matrix

$$D^k \doteq \rho \cdot (K^k)^{-1} \begin{bmatrix} I & -I \\ 0 & 0 \\ 0 & 0 \end{bmatrix}. \quad (19)$$

Lemma 5 (Lipschitz constant of the subsystem QP):

Suppose Assumption 5 holds and let p^* denote a KKT point which satisfies Assumption 6. Form QP (6) at a primal-dual point p^k using the exact Hessian $H^k = \nabla_{zz}^2 L(z^k, \nu^k, \mu^k)$. Initialize Algorithm 1 with z_i^k and $E_i^\top \lambda^k$ for all $i \in \mathcal{S}$. Let $p^k \in \mathcal{B}(p^*, \varepsilon)$ with ε from Lemma 4. Then, the Lipschitz constant d_2 in (14) is given by

$$d_2 = \max_{p^k \in \mathcal{B}(p^*, \varepsilon)} \|D^k\|. \quad (20)$$

□

Proof: As discussed in the proof of Lemma 4, the active sets of NLP (5), QP (6), and the centralized subsystem QP in Step (8a) are equivalent for $p^k \in \mathcal{B}(p^*, \varepsilon)$. Moreover, strict complementarity, LICQ, and the stronger SOSOC version (12) hold at the subsystem QP solution (y^{l+1}, μ^{l+1}) for all $l \in \mathbb{N}_0$. In centralized form, the KKT system of the subsystem QPs in Step (8a) reads

$$\underbrace{\begin{bmatrix} H^k + \rho I & \nabla g^k & \nabla h_{\mathcal{A}}^k \\ \nabla g^{k\top} & 0 & 0 \\ \nabla h_{\mathcal{A}}^{k\top} & 0 & 0 \end{bmatrix}}_{=K^k} \begin{bmatrix} y^{l+1} \\ \nu^{l+1} \\ \mu_{\mathcal{A}}^{l+1} \end{bmatrix} = \begin{bmatrix} -\nabla f^k - \gamma^l + \rho z^l \\ -g^k + \nabla g^{k\top} z^k \\ -h_{\mathcal{A}}^k + \nabla h_{\mathcal{A}}^{k\top} z^k \end{bmatrix}.$$

Furthermore, $\mu_{\mathcal{I}}^{l+1} = 0$. The KKT matrix K^k is invertible for all $p^k \in \mathcal{B}(p^*, \varepsilon)$, because of LICQ and the stronger SOSOC condition (12), cf. [40, Lem. 16.1]. Rearranging thus yields

$$\begin{bmatrix} y^{l+1} \\ \nu^{l+1} \\ \mu_{\mathcal{A}}^{l+1} \end{bmatrix} = (K^k)^{-1} \begin{bmatrix} -\nabla f^k - \gamma^l + \rho z^l \\ -g^k + \nabla g^{k\top} z^k \\ -h_{\mathcal{A}}^k + \nabla h_{\mathcal{A}}^{k\top} z^k \end{bmatrix}.$$

Likewise,

$$\begin{bmatrix} y_{\text{QP}}^{k,*} \\ \nu_{\text{QP}}^{k,*} \\ \mu_{\mathcal{A}, \text{QP}}^{k,*} \end{bmatrix} = (K^k)^{-1} \begin{bmatrix} -\nabla f^k - \gamma_{\text{QP}}^{k,*} + \rho z_{\text{QP}}^{k,*} \\ -g^k + \nabla g^{k\top} z^k \\ -h_{\mathcal{A}}^k + \nabla h_{\mathcal{A}}^{k\top} z^k \end{bmatrix}$$

and hence

$$\begin{bmatrix} \Delta y^{l+1} \\ \Delta \nu^{l+1} \\ \Delta \mu_{\mathcal{A}}^{l+1} \end{bmatrix} = \underbrace{\rho \cdot (K^k)^{-1} \begin{bmatrix} I & -I \\ 0 & 0 \\ 0 & 0 \end{bmatrix}}_{=D^k} \Delta w^l. \quad (21)$$

Since $\mu_{\mathcal{I}}^{l+1} = \mu_{\mathcal{I}, \text{QP}}^{k,*} = 0$, we obtain (14) with d_2 given in (20). ■

Lemma 5 shows how to compute the constant d_2 which is required to evaluate c_2 in the sufficient iteration bound (11). We next compute the ADMM contraction factor a_w by showing that, inside $\mathcal{B}(p^*, \varepsilon)$, ADMM behaves like a stable Linear Time-Invariant (LTI) system. To this end, we first partition the top block rows of D^k defined in (19) as

$$\begin{bmatrix} I & 0 & 0 \end{bmatrix} D^k \doteq \begin{bmatrix} T^k & -T^k \end{bmatrix}$$

to obtain the block matrix $T^k \in \mathbb{R}^{n \times n}$. Then, we define the ADMM system matrix

$$A^k \doteq \begin{bmatrix} M_{\text{avg}} T^k & M_{\text{avg}}(I - T^k) \\ (I - M_{\text{avg}})T^k & (I - M_{\text{avg}})(I - T^k) \end{bmatrix}.$$

Lemma 6 (ADMM contraction factor): Suppose Assumption 5 holds and let p^* denote a KKT point which satisfies Assumption 6. Form QP (6) at a primal-dual point p^k using the exact Hessian $H^k = \nabla_{zz}^2 L(z^k, \nu^k, \mu^k)$. Initialize Algorithm 1 with z_i^k and $E_i^\top \lambda^k$ for all $i \in \mathcal{S}$. Let $p^k \in \mathcal{B}(p^*, \varepsilon)$ with ε from Lemma 4. Then, the ADMM iterations read

$$w^{l+1} - w_{\text{QP}}^{k,*} = A^k (w^l - w_{\text{QP}}^{k,*}). \quad (22)$$

Furthermore, the ADMM contraction factor $a_w < 1$ in (13) is given by

$$a_w = \max_{p^k \in \mathcal{B}(p^*, \varepsilon)} \|A^k\|. \quad (23)$$

□

Proof: Lemma 4 guarantees that the active set of the centralized subsystem QP stays constant for all $l \in \mathbb{N}_0$, if $p^k \in \mathcal{B}(p^*, \varepsilon)$. Thus, the subsystem QP error is given by (21). Rewriting the top block rows of (21) yields

$$\Delta y^{l+1} = \begin{bmatrix} T^k & -T^k \end{bmatrix} \Delta w^l. \quad (24)$$

Recall the error in the ADMM averaging step from (15),

$$\Delta z^{l+1} = M_{\text{avg}} (\Delta y^{l+1} + \Delta \gamma^l / \rho). \quad (25)$$

Inserting (24) into (25) yields

$$\Delta z^{l+1} = [M_{\text{avg}} T^k \quad M_{\text{avg}}(I - T^k)] \Delta w^l. \quad (26)$$

By rearranging the dual update (8c), we obtain

$$\Delta \gamma^{l+1} / \rho = \Delta \gamma^l / \rho + (\Delta y^{l+1} - \Delta z^{l+1})$$

and hence

$$\frac{\Delta \gamma^{l+1}}{\rho} = [(I - M_{\text{avg}})T^k \quad (I - M_{\text{avg}})(I - T^k)] \Delta w^l. \quad (27)$$

By combining (26) and (27), we can write ADMM as the LTI system

$$\Delta w^{l+1} = \underbrace{\begin{bmatrix} M_{\text{avg}} T^k & M_{\text{avg}}(I - T^k) \\ (I - M_{\text{avg}}) T^k & (I - M_{\text{avg}})(I - T^k) \end{bmatrix}}_{A^k} \Delta w^l$$

to obtain (22). Moreover,

$$\|\Delta w^{l+1}\| \leq \|A^k\| \|\Delta w^l\|.$$

The q-linear ADMM convergence (13) yields

$$\|A^k\| = \max_{\Delta w^l \neq 0} \frac{\|A^k \Delta w^l\|}{\|\Delta w^l\|} = \max_{\Delta w^l \neq 0} \frac{\|\Delta w^{l+1}\|}{\|\Delta w^l\|} < 1$$

for all $p^k \in \mathcal{B}(p^*, \varepsilon)$. Finally, we obtain the worst-case ADMM contraction factor a_w inside $\mathcal{B}(p^*, \varepsilon)$ via (23). ■

Remark 3 (Multiple ADMM iterations per QP):

Convergence of the inexact SQP scheme is guaranteed if the approximate QP solutions satisfy (9). This condition requires a sufficiently accurate guess for the primal-dual variables p . While ADMM is q-convergent in w , it only is r-convergent in p . Hence in applications multiple ADMM iterations per SQP step are required to guarantee (9). □

C. Optimizer Convergence with Limited Inner Iterations

We now combine the outer convergence from Lemma 3 with the inner convergence from Lemma 4 to prove the q-linear convergence of Algorithm 2 for fixed l_{\max} .

Theorem 1 (dSQP convergence): Suppose Assumption 5 holds and let p^* denote a KKT point which satisfies Assumption 6. Form QP (6) with the exact Hessian $H^k = \nabla_{zz}^2 L(z^k, \nu^k, \mu^k)$. Let $0 < a < \bar{a}_p < 1$. Then there exists a constant $\varepsilon > 0$ such that the following holds with d_2 and a_w computed via (20) and (23).

If $p^0 \in \mathcal{B}(p^*, \varepsilon)$ and if the number l_{\max} of ADMM iterations per SQP iterations satisfies (11), then the sequence $\{p^k\}$ generated by Algorithm 2 converges to p^* and, for all $k \in \mathbb{N}_0$, satisfies $\|p^{k+1} - p^*\| \leq \bar{a}_p \|p^k - p^*\|$. □

Proof: By the outer convergence result (Lemma 3), there exists $\varepsilon_2 > 0$ such that the following holds. If the ADMM solutions to QP (6) satisfy the sufficient accuracy requirement (9) for the inexact SQP scheme and if $p^0 \in \mathcal{B}(p^*, \varepsilon_2)$, then the sequence $\{p^k\}$ generated by Algorithm 2 converges q-linearly to p^* . Let $\varepsilon \leq \varepsilon_2$. From the inner convergence (Lemma 4), there exists a radius $\varepsilon > 0$ such that the ADMM solutions satisfy (9) for all $p^k \in \mathcal{B}(p^*, \varepsilon)$. Thus, we obtain q-linear convergence in the outer iterations. ■

Remark 4 (Relation to [28]): An earlier version of dSQP is presented in [28]. There, an inexact Newton-type stopping criterion terminates ADMM dynamically in each SQP step and control applications were not considered. Theorem 1 guarantees convergence when the number of ADMM iterations per SQP iteration is fixed to l_{\max} . This avoids the online communication of convergence flags and allows us to use dSQP in the proposed decentralized RTI scheme. Consequently, the convergence proof derived in this article differs from [28] and, inspired by a centralized inexact SQP

scheme from [38], is centered around inequality (9) instead of inexact Newton methods. □

V. DECENTRALIZED REAL-TIME ITERATIONS

We now combine the q-linear convergence of dSQP and the RTI stability result from Lemma 1.

Consider the setpoint stabilization for the network \mathcal{S} of dynamical systems with dynamics (1b). In each control sampling interval δ , the state $x(t)$ is assumed to be measured and a constant input signal is applied to the system. We define the distributed NMPC control law $\kappa_d : \mathbb{R}^{n_x} \times \mathbb{R}^{n_p} \rightarrow \mathbb{R}^{n_u}$ as the map from the centralized state $x(t)$ and the dSQP initialization $p^0(t)$ to the first part $\bar{u}^{k_{\max}}(0)$ of the centralized input trajectory which is returned by Algorithm 2 with settings $k_{\max} \in \mathbb{N}$ and $H_i = \nabla_{z_i z_i}^2 L_i$. That is, in each NMPC step we apply dSQP with one or more outer iterations and with l_{\max} inner iterations per outer iteration to OCP (1), or respectively its NLP reformulation (5). Furthermore, we initialize dSQP with the OCP solution obtained in the previous NMPC step. Thus, the centralized system (2b) and dSQP form the closed-loop system optimizer dynamics (4), where Φ maps the current state $x(t)$ and dSQP output $p^{k_{\max}}(t)$ to the dSQP solution at the next time step. We are now ready to state our main result.

Theorem 2 (Decentralized RTI stability): Suppose that Assumptions 1 and 4 hold and that $\bar{p}(0) = 0$. Further assume, for all $x \in \mathbb{X}_{\bar{V}}$, that Assumption 5 holds and that $\bar{p}(x)$ satisfies Assumption 6. Consider $a \in (0, 1)$. For all $x \in \mathbb{X}_{\bar{V}}$, denote the dSQP convergence radius and contraction factor from Theorem 1 by $\varepsilon(x)$ and $\bar{a}_p(x)$, compute the constants $d_2(x)$ and $a_w(x)$ according to Lemmas 5 and 6, and assume the number of inner iterations l_{\max} satisfies (11). Let $\hat{r}_p = \min_{x \in \mathbb{X}_{\bar{V}}} \varepsilon(x)$ and $\bar{a}_p = \max_{x \in \mathbb{X}_{\bar{V}}} \bar{a}_p(x)$, compute $\bar{\delta}$ and \hat{r}_p via (29), and suppose the control sampling interval satisfies $\delta \leq \bar{\delta}$. Then, the following holds.

If the initial state $x(0) \in \mathbb{X}_{\bar{V}}$ and if Algorithm 2 is initialized with $p^0(0) \in \mathcal{B}(\bar{p}(x(0)), \hat{r}_p)$ in the first NMPC step, then the origin is a locally exponentially stable equilibrium of the closed-loop system-optimizer dynamics (4). □

Proof: Consider the reformulation of OCP (2) as a partially separable NLP (5). According to the dSQP convergence Theorem 1, Algorithm 2 converges q-linearly to the primal-dual solution $\bar{p}(x(t))$ for any initialization $p^0(t) \in \mathcal{B}(\bar{p}(x(t)), \hat{r}_p)$ and for all $x \in \mathbb{X}_{\bar{V}}$. Hence, dSQP satisfies the q-linear convergence Assumption 3. The Lipschitz continuity of the map \bar{p} follows from Assumption 6 via the BST [39, Thm. 3.2.2], because the functions in NLP (5) are twice continuously differentiable and because ∇g is continuously differentiable with respect to $x(t)$. That is, Assumption 2 holds. The exponential stability of the origin for the closed-loop system-optimizer dynamics therefore follows from Lemma 1. ■

Remark 5 (Region of attraction): The estimate region of attraction of the system-optimizer dynamics (4) is [7]

$$\Sigma \doteq \left\{ (x, p) \in \mathbb{R}^{n_x + n_p} \mid x \in \mathbb{X}_{\bar{V}}, \|p - \bar{p}(x)\| \leq \hat{r}_p \right\}.$$

The set $\mathbb{X}_{\bar{V}} = \{x \in \mathbb{R}^{n_x} \mid V(x) \leq \bar{V}\}$ is the level set over which Assumptions 1, 4, 5, and 6 hold and \tilde{r}_p can be computed via (29). \square

Remark 6 (Continuity of V , \sqrt{V} , and \bar{p}): Assumption 1 requires that V is continuous for all $x \in \mathbb{X}_{\bar{V}}$ and that \sqrt{V} is Lipschitz continuous at the origin. These conditions hold if V is Lipschitz continuous over $\mathbb{X}_{\bar{V}}$ and twice continuously differentiable at the origin [7]. This is the case if Assumption 6 holds for all $x \in \mathbb{X}_{\bar{V}}$ [39, Thm. 3.4.1]. The Lipschitz continuity of \bar{p} in Assumption 2 follows from the differentiability Assumption 5 and the regularity Assumption 6 via [39, Thm. 3.2.2]. \square

Remark 7 (Stability close to global optima): The careful reader will have noticed that the stability result of Theorem 2 requires the optimizer initialization to be close to the global minimum of the OCP. This assumption carries over from the centralized result [7, Thm. 25], which we invoke to prove stability. In practice, one will only obtain local minima for non-convex NLPs. However, we observe stability in simulations despite the convergence to local minima. To the best of our knowledge, centralized and decentralized RTI stability guarantees which only require optimizer initializations close to local minima are yet unavailable. \square

Remark 8 (Relation to [19]): Real-time distributed NMPC is also addressed in [19] and we comment on similarities and differences to our approach. Both schemes share three important properties: First, they do not require a coordinator. Second, they apply an a-priori fixed number of optimizer iterations in each NMPC step to find a suboptimal control input. Third, the optimizer contraction for subsequent NMPC steps is proven via two key ingredients: (a) q-linear optimizer convergence for sufficiently many inner iterations, i.e., l_{\max} ADMM iterations per SQP step for dSQP and M primal iterations for Algorithm 1 in [19], where M is in the notation of [19], and (b), sufficient proximity between subsequent state measurements, i.e., by choosing the sampling interval sufficiently small or by direct assumption [19].

On the other hand, the schemes differ in the employed optimization algorithm, in the order in which computations are executed on the subsystems, and in the obtained convergence result. The computationally expensive Step 3 in ADMM can be executed by all subsystems in parallel. In contrast, the decomposition scheme in [19] assigns subsystems into groups and the groups execute computation steps in sequence. And whereas Theorem 2 proves the local exponential stability of system and optimizer, [19, Thm. 5] bounds the optimizer suboptimality in closed-loop without addressing the system asymptotics. However, we invoke the more recent stability results from [7] to prove stability. Due to the q-linear optimizer convergence of Algorithm 1 of [19], we conjecture that Theorem 2 also holds under suitable assumptions if dSQP is replaced with the approach from [19]. \square

Remark 9 (Application to linear-quadratic DMPC): If NLP (5) is a convex QP, dSQP reduces to ADMM. In this case, the q-linear convergence of ADMM yields closed-loop stability for $l_{\max} \geq 1$ and sampling intervals below $\bar{\delta}$. This

follows from Lemma 1 by replacing the convergence in p in Assumption 3 with the ADMM convergence (13), cf. [38]. \square

A. Implementation Aspects

We next comment on the communication requirements of the proposed RTI scheme and on the choice of a suitable Hessian for constructing QP (6).

With respect to communication, the decentralized RTI scheme requires each subsystem to exchange messages with all neighbors in order to execute Step 4 of Algorithm 1. All other steps in ADMM and dSQP can be carried out without communication. As mentioned in Remark 2, this decentralized ADMM implementation is due to the fact that Step 4 is equivalent to an averaging procedure [34, Ch. 7]. Essentially, the step requires each subsystem to exchange predicted state trajectories with neighbors, compute an averaged state trajectory, and then to exchange the averaged trajectories with neighbors. Details about the implementation of the averaging procedure in a DMPC context are provided in [16, 29]. In this context, we comment on the relation between the dual variables λ and γ . Observe that λ is implicitly updated by ADMM in (8b), but only appears in the initialization Step 1 of Algorithm 2. Apart from this initialization, λ is only needed in the theoretical convergence analysis and not in the implementation of dSQP. This facilitates the averaging step for computing z^{l+1} as outlined in Appendix II, where the explicit computation of λ^{l+1} is omitted. ADMM ensures $\gamma_i^{l+1} = E_i^T \lambda^{l+1}$ for all $i \in \mathcal{S}$ and for all $k, l \in \mathbb{N}_0$. This can be used in closed-loop control to warm start γ_i^0 in Step 1 of dSQP with $\gamma_i^{k_{\max}}$ from the previous NMPC step. Thus, an initialization λ^0 is only required in the first control step. Possible initializations for the first control step that often work well are $\lambda^0 = 0$ or $\lambda^0 = \lambda^*$, if available.

With respect to the Hessian, the stability analysis holds for the exact Hessian $H_i = \nabla_{z_i z_i}^2 L_i$, because this guarantees local q-linear convergence of dSQP such that the controller meets Assumption 3. However, the exact Hessian may not always be a favorable choice, because $\nabla_{z_i z_i}^2 L_i$ can be indefinite outside the dSQP convergence region $\mathcal{B}(p^*, \varepsilon)$ and because $\nabla_{z_i z_i}^2 L_i$ must be evaluated in each dSQP iteration. Instead, the Constrained Gauss-Newton (CGN) method, first introduced as the generalized Gauss-Newton method [42], provides an alternative which is often effective in NMPC [43]. Consider a specialized version of NLP (5) with least squares objectives

$$f_i(z_i) = \frac{1}{2} \|M_i z_i - m_i\|_2^2, \quad (28)$$

where the matrices $M_i \in \mathbb{R}^{n_i \times n_i}$ are positive definite and the vectors $m_i \in \mathbb{R}^{n_i}$ are constants for all $i \in \mathcal{S}$. Such objectives commonly occur in NMPC for setpoint stabilization, see Section VI. The CGN method builds QP (6) with the Gauss-Newton (GN) Hessian approximation $H_i = B_i \doteq M_i^T M_i$ for all $i \in \mathcal{S}$. Crucially, the matrices B_i are constant, positive definite, and can be evaluated offline.

However, stability guarantees for our proposed RTI scheme when using the GN Hessian are yet unavailable.

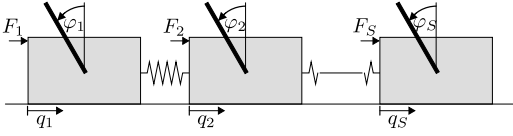


Fig. 1: Coupled inverted pendulums on carts.

While the CGN method is locally guaranteed to converge q -linearly in some norm [43], the convergence is not necessarily q -linear in the Euclidean norm $\|p^k - p^*\|$. This impedes a straight-forward stability proof via Lemma 1 as Assumption 3 may not hold.

VI. NUMERICAL RESULTS

We consider the setpoint stabilization of coupled inverted pendulums. Each pendulum is attached to a cart and the carts are coupled via springs as shown in Figure 1. Let q_i be the cart position and φ_i be the angular deviation from the upright position for pendulum i . The state of pendulum i is $x_i = (q_i, \dot{q}_i, \varphi_i, \dot{\varphi}_i) \in \mathbb{R}^4$ and the input is the force $u_i = F_i \in [-100 \text{ N}, 100 \text{ N}]$ applied to the cart. The carts are connected in a chain where each cart is coupled to its neighbors via a spring with stiffness $k = 0.1 \text{ N/m}$. Let $M_c = 2 \text{ kg}$ and $m = 0.25 \text{ kg}$ denote the masses of each cart and pendulum, respectively, let $l = 0.2 \text{ m}$ denote the length of each pendulum, and denote the gravity of earth by $g = 9.81 \text{ m/s}^2$. The continuous-time equations of motion of pendulum i read $\ddot{q}_i = (u_i + \frac{3}{4}mg \sin(\varphi_i) \cos(\varphi_i) - \frac{ml}{2} \dot{\varphi}_i^2 \sin(\varphi_i) + F_i^{\text{left}} + F_i^{\text{right}}) / (M_c + m - \frac{3}{4}m(\cos(\varphi_i))^2)$ and $\ddot{\varphi}_i = \frac{3g}{2l} \sin(\varphi_i) + \frac{3}{2l} \cos(\varphi_i) \dot{q}_i$. If applicable, the coupling forces are $F_i^{\text{left}} \doteq k(q_{i-1} - q_i)$ and $F_i^{\text{right}} \doteq k(q_{i+1} - q_i)$. We discretize the continuous-time dynamics using the explicit Runge-Kutta fourth-order method (RK4) with a shooting interval $h = 40 \text{ ms}$ and obtain the discrete-time model $f_i^h : \mathbb{R}^4 \times \mathbb{R} \times \mathbb{R}^{n_{\text{in}}} \rightarrow \mathbb{R}^4$. For this discretization, we not only keep the control u_i constant over the integration step, but also the neighboring positions q_{i-1} and q_{i+1} when evaluating the system dynamics. This simplification preserves the coupling structure, i.e., the discrete-time dynamics of each subsystem only depend on the left and right neighbors. However, the trade-off associated with this simplification is that the integration order with respect to the neighboring states reduces to one. A more accurate alternative is the distributed multiple shooting scheme [44] which expresses the state trajectories as linear combinations of basis functions, e.g., Legendre polynomials, and matches the basis function coefficients between neighboring subsystems.

A. Optimal Control Problem Design

We design OCP (1) such that the value function is a Lyapunov function which satisfies inequalities (3). For the sake of reducing the computational burden, our design does not enforce a terminal constraint in the OCP [32]. Thus, for the pendulum example, all inequality constraints are input constraints. However, if desired, terminal constraints

could also be considered. We choose separable quadratic stage costs $\ell_i(x_i, u_i) = x_i^\top Q_i x_i / 2 + u_i^\top R_i u_i / 2$, where we set $R_i = 0.001$ and take $Q_i = \text{diag}(1, 10^{-4}, 10, 10^{-4})$ from [45]. We further design $V_{f,i}(x_i) = \beta_2 x_i^\top P_i x_i / 2$, where we find $\beta_2 \geq 1$ and $P_i \in \mathbb{R}^{4 \times 4}$ as follows. First, we neglect coupling between neighbors, discretize the dynamics with RK4 at sampling interval $\delta = 40 \text{ ms}$, and linearize at the origin to obtain a model (A_i, B_i) with $A_i \in \mathbb{R}^{4 \times 4}$ and $B_i \in \mathbb{R}^{4 \times 1}$ for all $i \in \mathcal{S}$. This allows to solve the algebraic Riccati equation

$$P_i = A_i^\top P_i A_i - (A_i^\top P_i B_i)(R_i + B_i^\top P_i B_i)^{-1} (B_i^\top P_i A_i) + Q_i$$

individually for each subsystem to obtain P_i and the terminal control law $u_i = K_i x_i$, where $K_i \doteq -(B_i^\top P_i B_i + R_i)^{-1} (B_i^\top P_i A_i)$. Next, we discretize the centralized dynamics f^c including coupling with RK4 at $\delta = 40 \text{ ms}$ and linearize at the origin to obtain the centralized system (A, B) with $A \in \mathbb{R}^{4S \times 4S}$ and $B \in \mathbb{R}^{4S \times S}$. For the example at hand, the terminal controller $K = \text{diag}(K_1, \dots, K_S)$ also stabilizes the coupled centralized system, i.e., the matrix $A_K = A + BK$ is Schur stable. Denote the centralized weight matrices as $Q \doteq \text{diag}(Q_1, \dots, Q_S)$, $R \doteq \text{diag}(R_1, \dots, R_S)$, and $P \doteq \text{diag}(P_1, \dots, P_S)$ and define $Q_K \doteq Q + K^\top R K$. To meet the sufficient decrease condition

$$V_f(f^\delta(x, Kx)) - V_f(x) \leq -\ell(x, Kx),$$

we increase β_2 until the matrix $\Delta Q \doteq \tilde{Q} - Q_K$ is positive definite, where $\tilde{Q} \doteq \beta_2(P - A_K^\top P A_K) / \mu$ and where the parameter μ is in the notation of [46, Sec. 2.5.5]. We set $\mu = 1.01$ and obtain $\beta_2 = 1.1$.

Remark 10 (Decentralized V_f design): The matrices P_i and terminal controllers K_i are computed by neglecting the coupling of the dynamics and by solving the Riccati equation for each subsystem individually. This simplification is not guaranteed to stabilize coupled linearized systems in general, but the design stabilizes the chain of pendulums considered here. Hence, the matrix ΔQ is positive definite for sufficiently large β_2 . A similar design approach is suggested in [17, Remark 4]. More elaborate decentralized linear-quadratic control designs can be found in the classic textbook [3]. \square

B. Swing-up Simulation

We consider the swing up of $S = 20$ pendulums to analyze the efficacy of the proposed RTI scheme. Our Matlab implementation uses CasADi to evaluate the derivatives in Step 3 of dSQP [47]. The quadratic subproblems in Step 3 of ADMM are solved using OSQP with tolerances $\epsilon_{\text{abs}} = \epsilon_{\text{rel}} = \epsilon_{\text{prim}} = \epsilon_{\text{dual}} = 10^{-8}$, where the tolerances are in the notation of [48]. After the control input is computed in each NMPC step, the centralized system is simulated using RK4 with integration step size equal to the control sampling interval δ to obtain the system state at the next sampling instant. We select the penalty parameter ρ of ADMM from the set $\{0.1, 1, 10, 100\}$ and choose $\rho = 1$.

We compare three test cases with varying initial conditions, OCP designs, and solver settings as summarized in

Table I. The pendulums initially rest in the lower equilibrium position $x_i(0) = (q_i(0), 0, \pi, 0)$, where the initial cart displacement is given in Table I. The goal is to steer all pendulums to the upright equilibrium position at $x_i = 0$. The OCP is designed with quadratic weights as described in Subsection VI-A. The time horizon is chosen as $T = 0.4$ s and the scaling factor in the objective is set to $\beta = 1$. The further parameters in Table I are the shooting interval h in the OCP, the discrete-time horizon $N = T/h$, the chosen Hessian for QP (6), the maximum number of SQP iterations per NMPC step k_{\max} , the maximum number of ADMM iterations per SQP iteration l_{\max} , the total number of decision variables in the centralized OCP n , the total number of subsystem equality constraints n_g , the total number of subsystem inequality constraints n_h , and the number of consensus constraints n_c . For all cases, the control sampling interval is set to $\delta = 40$ ms. For cases one and two, we choose the exact Hessian if $\nabla_{z_i z_i}^2 L_i$ is positive definite and otherwise we select the GN Hessian. For case three, we always choose the GN Hessian approximation. A quadratic penalty term with weight 10^{-5} is added to the objective (1a) for all state copies to meet Assumption 6 (ii). We initialize dSQP in the first NMPC step at a solution found by `ipopt` [49]. In all subsequent NMPC steps, we initialize dSQP with the solution produced in the previous control step.

Table II summarizes the simulation results. We analyze the averaged closed-loop control performance

$$J_{\text{cl}} \doteq \frac{1}{T_f} \sum_{t=0}^{t_n} \sum_{i \in \mathcal{S}} \delta \cdot \ell_i(x_i(t), u_i(t)),$$

where T_f is the duration of each simulation and t_n is the number of NMPC steps per simulation. Furthermore, we analyze the dSQP execution time per NMPC step on a desktop computer. We run each test case ten times to account for varying execution times in between runs and we take two different types of time measurements in each NMPC step. In the first type, we measure the total execution time of one call to dSQP, which is summarized in the second and third columns from the left in Table II. This includes running the specified number of SQP and ADMM iterations for all pendulums in series as well as the costly creation and destruction of intermediate data structures. This is due to the prototypical nature of our Matlab implementation and would be avoided in embedded applications. In the second type of time measurement, summarized in columns four to six of Table II, we measure only imperative code blocks that cannot be avoided in an efficient implementation, and we take measurements for each subsystem individually. This includes calls to `CasADi` for evaluating derivatives, calls to `OSQP` for updating and solving QPs in ADMM, and computing Steps 4–5 of ADMM. Column six summarizes the percentage of per-subsystem solve times that were below the sampling interval.

The closed-loop system and optimizer trajectories are shown in Figures 2–4. The top three plots in each figure display the cart positions, pendulum angles, and control

TABLE I: Test case specifications. All cases consider a sampling interval $\delta = 40$ ms.

Case	$q_i(0)$	h [ms]	N	H	k_{\max}	l_{\max}	n	n_g	n_h	n_c
1	-1°	40	10	exact	1	6	1518	880	440	418
2	i	40	10	exact	3	6	1518	880	440	418
3	i	57	7	GN	2	3	1104	640	320	304

TABLE II: Computation times per NMPC step and closed-loop performance J_{cl} for a prototypical Matlab implementation. The fast computation times in test cases one and three demonstrate the real-time feasibility of decentralized real-time iterations.

Case	all subsystems combined		per subsystem		$\leq \delta$	J_{cl}
	median [ms]	max. [ms]	median [ms]	max. [ms]		
1	239.07	448.19	12.03	29.24	100 %	65.86
2	697.04	2394.02	35.10	210.38	93.54 %	156.05
3	227.06	746.51	10.76	60.25	99.90 %	180.66

inputs. The optimizer evolutions in the bottom plots show the convergence of dSQP to the OCP solutions p^* found by `ipopt`.

In all test cases, the pendulums reach the upright equilibrium position while satisfying the input constraints. The initial cart displacements in the first test case are less challenging than in the second case. In fact, the increase in k_{\max} from the first to the second test case is necessary for a successful swing up due to the different initial conditions. That is, the optimizer settings of case one do not provide stability in simulation for case two. While the per-subsystem computation time in the first test case is below the sampling interval δ , the computation time of the second test case would not be real-time feasible.¹ Therefore, we increase the shooting interval in the third test case to reduce the OCP size and we select the GN Hessian to reduce the time spent evaluating derivatives such that case three requires less iterations per NMPC step for a successful swing up. On the other hand, this reduces performance as can be seen from the prolonged settling time and the increase in J_{cl} . Choosing a shooting interval $h > \delta$ is a well-known technique for reducing RTI computation times [4]. However, the stability guarantees provided by Theorem 2 only hold if $h = \delta$ and if the exact Hessian is chosen.

The time measurements, obtained for a prototypical Matlab implementation, show that the per-subsystem computation times are mostly below the control sampling interval. This does not imply that an efficient decentralized implementation would necessarily be real-time feasible, in particular if communication latencies add to the computation time.² However, the obtained computation times indicate that control sampling intervals in the millisecond range are conceivable via the decentralized RTI scheme.

¹Non-negligible computation times below the sampling interval can be compensated by solving the OCP for the subsequent control input [50].

²Latency measurements for a decentralized dSQP implementation indicate that a worst-case latency of approximately 10 ms can be expected for running $k_{\max} = 1$ SQP and $l_{\max} = 6$ ADMM iterations in a laboratory setting [29].

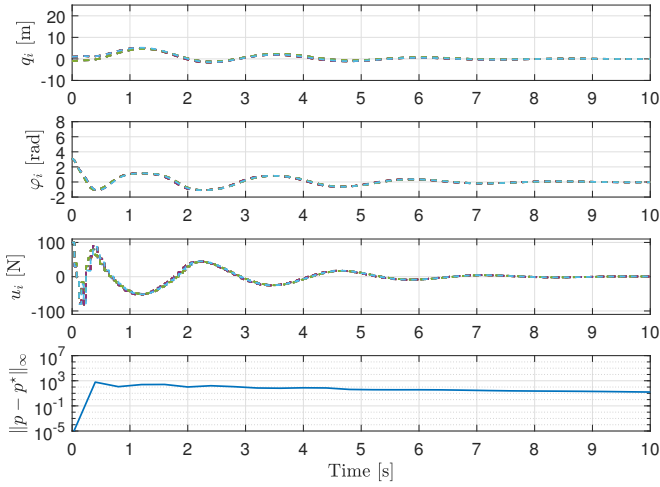


Fig. 2: Test case 1: closed-loop system and optimizer convergence with 6 ADMM iterations per NMPC step.

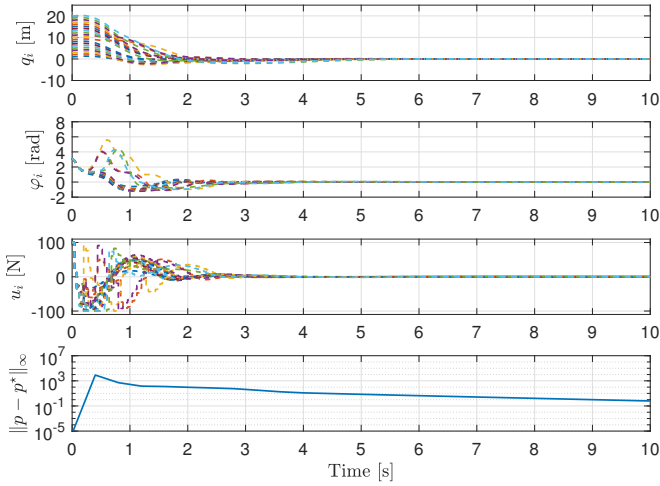


Fig. 3: Test case 2: closed-loop system and optimizer convergence for a challenging initial condition with 18 ADMM iterations per NMPC step.

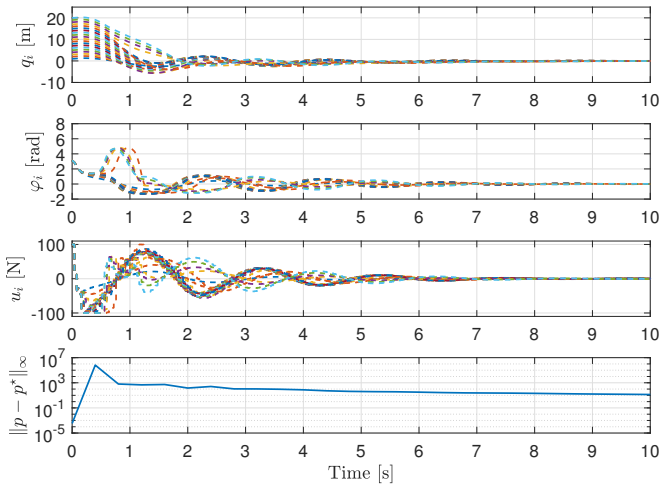


Fig. 4: Test case 3: closed-loop system and optimizer convergence with 6 ADMM iterations per NMPC step.

C. Parameter estimation and validity of assumptions

The OCP design discussed in subsection VI-A meets the value function requirements (3) in Assumption 1 and the pendulum dynamics satisfy Assumption 4. Numerical a-posteriori analyses further show that the KKT points found by `ipopt` satisfy the regularity Assumption 6 if the system is close to the setpoint. The continuity conditions in Assumptions 1 and 2 thus hold for the identified local minima. Finally, Assumption 5 is satisfied, because the pendulum dynamics are sufficiently smooth.

The bounds (11) on the ADMM iterations l_{\max} and (29) on $\bar{\delta}$ offer a compromise between optimality, i.e., large l_{\max} , and sampling frequency, i.e., small $\bar{\delta}$. To obtain stability for a large sampling interval $\bar{\delta}$ via (29), the outer contraction factor a_p must be small. By Theorem 1, this requires a to be small, which results in more ADMM iterations l_{\max} via (11). That is, for low sampling frequencies, ADMM must solve the SQP subproblems to greater accuracy. To estimate the number of ADMM iterations l_{\max} sufficient to guarantee stability for the sampling interval $\delta = 40$ ms chosen in the simulations, we proceed as follows: We estimate the constants for calculating δ_5 in Appendix I via simulations close to the setpoint with the ideal centralized NMPC feedback law $\kappa(x)$ using IPOPT, similarly to [7]. These simulations yield constants $a_1 = 0.5326$, $a_2 = 7.1530$, $a_3 = 0.2113$, $L_{f,x}^c = 86.2704$, $L_{f,u}^c = 3.6685$, $L_{p,x} = 51.3647$, $L_{V,x} = 1.7908$, and $L_{V,p} = 207.1090$. Then, the QP approximation of the OCP at the setpoint yields $c_1 = 1.7321$ and $c_2 = 251.5737$. Finally, we sample the ADMM LTI dynamics (22) in simulations for random w and obtain $a_w = 0.9989$. As a result, $l_{\max} = 24007$ ADMM iterations are sufficient to guarantee stability for $\delta_5 = 40$ ms. Compared with the settings in Table I, this estimate is quite conservative. Here, the conservatism primarily stems from the Lipschitz constants in the system dynamics and the contraction factor a_w . In hardware experiments and simulations, we observe good control performance already for 2–30 ADMM iterations per MPC step, depending on the application [29–31].

VII. CONCLUSION

This paper has presented a novel decentralized RTI scheme for distributed NMPC based on dSQP. The proposed scheme applies finitely many optimizer iterations per control step and does not require subsystems to exchange information with a coordinator. Stability guarantees are proven for the system-optimizer dynamics in closed loop by combining centralized RTI stability guarantees with novel dSQP convergence results. Numerical simulations demonstrate the efficacy of the proposed scheme for a chain of coupled inverted pendulums. Future work will consider further mechatronic systems and hardware experiments.

APPENDIX I CENTRALIZED RTI STABILITY

This section summarizes the steps for computing the sufficient sampling interval $\bar{\delta} > 0$ and optimizer initialization radius $\tilde{r}_p > 0$ which guarantee stability of centralized

RTI [7]. First, we recall the following two results which yield constants $r_x, r_p, \delta_1 > 0$.

Lemma 7 (Optimizer perturbation [7]): Let Assumptions 2 and 3 hold. Then, there exist positive constants $r_x \leq \hat{r}_x$ and $r_p \leq \hat{r}_p$ such that $\|p^{k+1} - \bar{p}(x')\| \leq a_p \|p^k - \bar{p}(x)\| + L_{p,x} a_p \|x' - x\|$ for all $x \in \mathbb{X}_{\bar{V}}, p \in \mathcal{B}(\bar{p}(x), r_z)$, and $x' \in \mathcal{B}(x, r_x)$. \square

Lemma 8 (Lipschitz discrete-time dynamics [7]): Let Assumption 4 hold. Then, there exists a positive finite constant δ_1 such that, for all $x \in \mathbb{X}_{\bar{V}}, p \in \mathcal{B}(\bar{p}(x), r_p)$, and $\delta \leq \delta_1$,

$$\|f^\delta(x, M_{u,p}p) - x\| \leq \delta \cdot \left(L_{f,x}^{\delta_1} \|x\| + L_{f,u}^{\delta_1} \|M_{u,p}p\| \right),$$

where $L_{f,x}^{\delta_1} \doteq e^{L_{f,x}^c \delta_1} L_{f,x}^c$ and $L_{f,u}^{\delta_1} \doteq e^{L_{f,u}^c \delta_1} L_{f,u}^c$. \square

Furthermore, define the constants $\eta \doteq L_{f,x}^{\delta_1} + L_{f,u}^{\delta_1} L_{p,x}$, $r_{\bar{V}} \doteq (\bar{V}/a_1)^{1/2}$,

$$\delta_3 \doteq \min \left\{ \delta_0, \delta_1, \frac{r_x}{\eta r_{\bar{V}} + L_{f,u}^{\delta_1} r_p}, \frac{r_p(1-a_p)}{L_{p,x} a_p (L_{f,u}^{\delta_1} r_p + \eta r_{\bar{V}})} \right\},$$

$$\kappa \doteq a_p \left(1 + \delta_3 L_{p,x} L_{f,u}^{\delta_1} \right), \quad L_V \doteq 2\bar{V}^{1/2} L_{V,x},$$

$$\bar{a} \doteq a_3/a_2, \quad L_e \doteq L_V L_{f,u}^{\delta_1}, \quad L_{V,p} \doteq L_{f,u}^c e^{\delta_1 L_{f,x}^c} L_{V,x},$$

$$\beta \doteq (\bar{a}\sqrt{a_1})/(4L_{p,x} a_p \eta),$$

$$\delta'_4 \doteq \frac{(1-\kappa)\tilde{r}_p\sqrt{a_1}}{\bar{V}^{1/2} L_{p,x} a_p \eta}, \quad \text{and} \quad \delta_5 \doteq \frac{\beta(1-\kappa)}{L_{V,p}}.$$

The sampling interval $\bar{\delta}$ and optimizer initialization radius \tilde{r}_p sufficient for closed-loop stability read [7]

$$\bar{\delta} \doteq \min\{\delta_3, \delta'_4, \delta_5\} \quad \text{and} \quad \tilde{r}_p \doteq \min\{r_p, \bar{a}\bar{V}/L_e\}. \quad (29)$$

APPENDIX II

NLP FORMULATION AND DECENTRALIZED ADMM

This section presents an example to demonstrate the reformulation of OCP (2) as a partially separable NLP (5) and the decentralization of the ADMM averaging step.

Example 1 (OCP as partially separable NLP [20]):

Consider a set $\mathcal{S} = \{1, 2\}$ of subsystems with $x_i, u_i \in \mathbb{R}$ for all $i \in \mathcal{S}$ governed by the dynamics

$$\begin{aligned} x_1(t+1) &= x_1(t) + u_1(t), & x_1(0) &= x_{1,0} \\ x_2(t+1) &= x_1(t) + x_2(t), & x_2(0) &= x_{2,0}. \end{aligned}$$

For a horizon $N = 1$, the decision variables in OCP (2) then read $\bar{x} \doteq (\bar{x}_1(0), \bar{x}_1(1), \bar{x}_2(0), \bar{x}_2(1))$ and $\bar{u} \doteq \bar{u}_1(0)$. To obtain a partially separable NLP, we define the state copy $\bar{v}_2 \doteq \bar{x}_1$ and the decision variables $z_1 \doteq (\bar{x}_1(0), \bar{x}_1(1), \bar{u}_1(0))$ and $z_2 \doteq (\bar{x}_2(0), \bar{x}_2(1), \bar{v}_2(0))$. The dynamics can be reformulated as subsystem constraints (5b),

$$\begin{aligned} g_1(z_1) &\doteq \begin{bmatrix} \bar{x}_1(0) + \bar{u}_1(0) - \bar{x}_1(1) \\ \bar{x}_1(0) - x_{1,0} \end{bmatrix} \\ g_2(z_2) &\doteq \begin{bmatrix} \bar{x}_2(0) + \bar{v}_2(0) - \bar{x}_2(1) \\ \bar{x}_2(0) - x_{2,0} \end{bmatrix}. \end{aligned}$$

The constraints (5d) couple original and copied states,

$$\underbrace{\begin{bmatrix} 1 & 0 & 0 \end{bmatrix}}_{\doteq E_1} z_1 + \underbrace{\begin{bmatrix} 0 & 0 & -1 \end{bmatrix}}_{\doteq E_2} z_2 = 0. \quad \square$$

Example 1 reformulates coupled dynamics. Coupled costs (1a) and constraints (1e) can be treated similarly.

The reformulation allows to decentralize ADMM as follows. The sparsity in E_1 and E_2 together with $c = 0$ allow to view NLP (5) as a so-called consensus problem, where each subsystem optimizes over a selection of the centralized decision variables (\bar{x}, \bar{u}) . Specifically for Example 1, Subsystem 1 optimizes over $(\bar{x}_1(0), \bar{x}_1(1), \bar{u}_1(0))$ and Subsystem 2 optimizes over $(\bar{x}_1(0), \bar{x}_2(0), \bar{x}_2(1))$. A derivation of the decentralized implementation of Step (8b) for general consensus problems is provided in [34, Ch. 7.2]. To make a closer connection to NLP (5), recall from the proof of Lemma 4 that the z -update in ADMM is given by $z^{l+1} = M_{\text{avg}}(y^l + \gamma^l/\rho)$. For Example 1, the ADMM averaging matrix M_{avg} reads

$$M_{\text{avg}} = I - E^\top (EE^\top)^{-1} E = \begin{bmatrix} 0.5 & 0 & 0 & 0 & 0 & 0.5 \\ 0 & 1 & 0 & 0 & 0 & 0 \\ 0 & 0 & 1 & 0 & 0 & 0 \\ 0 & 0 & 0 & 1 & 0 & 0 \\ 0 & 0 & 0 & 0 & 1 & 0 \\ 0.5 & 0 & 0 & 0 & 0 & 0.5 \end{bmatrix}.$$

That is, the update for the coupled variable $\bar{x}_1(0)$ is

$$[z_1]_1^{l+1} = [z_2]_3^{l+1} = \frac{[y_1]_1^{l+1} + [y_2]_3^{l+1} + ([\gamma_1]_1^l + [\gamma_2]_3^l)/\rho}{2}.$$

A common approach to decentralize ADMM in DMPC is to send the variables on the right hand side of to the above average to the subsystem with the original state, i.e., Subsystem 1 in Example 1. Then, the average is evaluated and the result is sent to the subsystems with the copied states, i.e., Subsystem 2 in Example 1. For more details, see [16, 29, 30].

REFERENCES

- [1] A. N. Venkat, I. A. Hiskens, J. B. Rawlings, and S. J. Wright, "Distributed MPC strategies with application to power system automatic generation control," *IEEE Trans. Control Syst. Technol.*, vol. 16, no. 6, pp. 1192–1206, 2008.
- [2] R. Van Parys and G. Pipeleers, "Distributed MPC for multi-vehicle systems moving in formation," *Rob. Auton. Syst.*, vol. 97, pp. 144–152, 2017.
- [3] D. D. Siljak, *Decentralized control of complex systems*. Academic Press, 1991.
- [4] M. Diehl, H. G. Bock, J. P. Schlöder, R. Findeisen, Z. Nagy, and F. Allgöwer, "Real-time optimization and nonlinear model predictive control of processes governed by differential-algebraic equations," *J Process Control*, vol. 12, no. 4, pp. 577–585, 2002.
- [5] V. M. Zavala and L. T. Biegler, "The advanced-step NMPC controller: Optimality, stability and robustness," *Automatica*, vol. 45, no. 1, pp. 86–93, 2009.
- [6] I. J. Wolf and W. Marquardt, "Fast NMPC schemes for regulatory and economic NMPC—a review," *J Process Control*, vol. 44, pp. 162–183, 2016.
- [7] A. Zanelli, Q. Tran-Dinh, and M. Diehl, "A Lyapunov function for the combined system-optimizer dynamics in inexact model predictive control," *Automatica*, vol. 134, p. 109901, 2021.
- [8] B. Käpernick and K. Graichen, "The gradient based nonlinear model predictive control software GRAMPC," in *Eur. Contr. Conf.*, 2014, pp. 1170–1175.
- [9] M. Schulze Darup, G. Book, and P. Giselsson, "Towards real-time ADMM for linear MPC," in *Eur. Contr. Conf.*, 2019, pp. 4276–4282.

- [10] R. Scattolini, "Architectures for distributed and hierarchical model predictive control – a review," *J Process Control*, vol. 19, no. 5, pp. 723–731, 2009.
- [11] M. A. Müller and F. Allgöwer, "Economic and distributed model predictive control: recent developments in optimization-based control," *SICE J. Control Meas. Syst. Integr.*, vol. 10, no. 2, pp. 39–52, 2017.
- [12] W. B. Dunbar, "Distributed receding horizon control of dynamically coupled nonlinear systems," *IEEE Trans. Autom. Control*, vol. 52, no. 7, pp. 1249–1263, 2007.
- [13] M. A. Müller, M. Reble, and F. Allgöwer, "Cooperative control of dynamically decoupled systems via distributed model predictive control," *Int. J. Robust Nonlinear Control*, vol. 22, no. 12, pp. 1376–1397, 2012.
- [14] P. Varutti, B. Kern, and R. Findeisen, "Dissipativity-based distributed nonlinear predictive control for cascaded systems," *IFAC Proceedings Volumes*, vol. 45, no. 15, pp. 439–444, 2012.
- [15] C. Conte, C. N. Jones, M. Morari, and M. N. Zeilinger, "Distributed synthesis and stability of cooperative distributed model predictive control for linear systems," *Automatica*, vol. 69, pp. 117–125, 2016.
- [16] A. Bestler and K. Graichen, "Distributed model predictive control for continuous-time nonlinear systems based on suboptimal ADMM," *Optim. Control. Appl. Methods*, vol. 40, no. 1, pp. 1–23, 2019.
- [17] B. T. Stewart, S. J. Wright, and J. B. Rawlings, "Cooperative distributed model predictive control for nonlinear systems," *J Process Control*, vol. 21, no. 5, pp. 698–704, 2011.
- [18] T. H. Summers and J. Lygeros, "Distributed model predictive consensus via the alternating direction method of multipliers," in *Allerton Conf. Comm. Contr. Comp.*, 2012, pp. 79–84.
- [19] J.-H. Hours and C. N. Jones, "A parametric nonconvex decomposition algorithm for real-time and distributed NMPC," *IEEE Trans. Autom. Control*, vol. 61, no. 2, pp. 287–302, 2016.
- [20] G. Stomberg, A. Engelmann, and T. Faulwasser, "A compendium of optimization algorithms for distributed linear-quadratic MPC," *at - Automatisierungstechnik*, vol. 70, no. 4, pp. 317–330, 2022.
- [21] D. P. Bertsekas and J. N. Tsitsiklis, *Parallel and Distributed Computation: Numerical Methods*. Englewood Cliffs, NJ: Prentice Hall, 1989, vol. 23.
- [22] A. Nedić, A. Olshevsky, and S. Wei, "Decentralized Consensus Optimization and Resource Allocation," in *Large-Scale and Distributed Optimization*, Springer, 2018, pp. 247–287.
- [23] G. Darivianakis, A. Eichler, and J. Lygeros, "Distributed model predictive control for linear systems with adaptive terminal sets," *IEEE Trans. Autom. Control*, vol. 65, no. 3, pp. 1044–1056, 2019.
- [24] J. Köhler, M. A. Müller, and F. Allgöwer, "Distributed model predictive control—recursive feasibility under inexact dual optimization," *Automatica*, vol. 102, pp. 1–9, 2019.
- [25] P. Giselsson and A. Rantzer, "On feasibility, stability and performance in distributed model predictive control," *IEEE Trans. Autom. Control*, vol. 59, no. 4, pp. 1031–1036, 2014.
- [26] A. Themelis and P. Patrinos, "Douglas–Rachford splitting and ADMM for nonconvex optimization: Tight convergence results," *SIAM J. Optim.*, vol. 30, no. 1, pp. 149–181, 2020.
- [27] Y. Wang, W. Yin, and J. Zeng, "Global convergence of ADMM in nonconvex nonsmooth optimization," *J. Sci. Comput.*, vol. 78, no. 1, pp. 29–63, 2019.
- [28] G. Stomberg, A. Engelmann, and T. Faulwasser, "Decentralized non-convex optimization via bi-level SQP and ADMM," in *IEEE Conf. Dec. Contr.*, 2022, pp. 273–278.
- [29] G. Stomberg, H. Ebel, T. Faulwasser, and P. Eberhard, "Cooperative distributed MPC via decentralized real-time optimization: Implementation results for robot formations," *Control Eng. Pract.*, vol. 138, p. 105 579, 2023.
- [30] G. Stomberg, R. Schwan, A. Grillo, C. N. Jones, and T. Faulwasser, "Cooperative distributed model predictive control for embedded systems: Experiments with hovercraft formations," in *arXiv*, 2024.
- [31] G. Stomberg, M. Raetsch, A. Engelmann, and T. Faulwasser, "Large problems are not necessarily hard: A case study on distributed NMPC paying off," *arXiv*, 2024.
- [32] D. Limón, T. Alamo, F. Salas, and E. F. Camacho, "On the stability of constrained MPC without terminal constraint," *IEEE Trans. Autom. Control*, vol. 51, no. 5, pp. 832–836, 2006.
- [33] P. Chanfreut, J. M. Maestre, and E. F. Camacho, "A survey on clustering methods for distributed and networked control systems," *Annu. Rev. Control*, vol. 52, pp. 75–90, 2021.
- [34] S. Boyd, N. Parikh, E. Chu, B. Peleato, and J. Eckstein, "Distributed optimization and statistical learning via the alternating direction method of multipliers," *Found. Trends Mach. Learn.*, vol. 3, no. 1, pp. 1–122, 2011.
- [35] A. Engelmann, Y. Jiang, B. Houska, and T. Faulwasser, "Decomposition of nonconvex optimization via bi-level distributed ALADIN," *IEEE Trans. Contr. Netw. Syst.*, vol. 7, no. 4, pp. 1848–1858, 2020.
- [36] P. T. Boggs and J. W. Tolle, "Sequential quadratic programming," *Acta Numer.*, vol. 4, pp. 1–51, 1995.
- [37] S. M. Robinson, "Perturbed Kuhn-Tucker points and rates of convergence for a class of nonlinear-programming algorithms," *Math. Program.*, vol. 7, pp. 1–16, 1974.
- [38] A. Zanelli, "Inexact methods for nonlinear model predictive control: Stability, application, and software," Ph.D. dissertation, University of Freiburg, 2021.
- [39] A. V. Fiacco, *Introduction to Sensitivity and Stability Analysis in Nonlinear Programming*, R. Bellman, Ed. Academic Press, 1983.
- [40] J. Nocedal and S. Wright, *Numerical Optimization*. Springer Science & Business Media, New York, 2006.
- [41] W. H. Yang and D. Han, "Linear Convergence of the Alternating Direction Method of Multipliers for a Class of Convex Optimization Problems," *SIAM J. Numer. Anal.*, vol. 54, no. 2, pp. 625–640, 2016.
- [42] H. G. Bock, "Recent advances in parameter identification techniques for ODE," in *Numerical Treatment of Inverse Problems in Differential and Integral Equations*, P. Deuffhard and E. Hairer, Eds., Boston, MA: Birkhäuser, 1983, pp. 95–121.
- [43] F. Messerer, K. Baumgärtner, and M. Diehl, "Survey of sequential convex programming and generalized Gauss-Newton methods," *ESAIM: Proc. Surv.*, vol. 71, pp. 64–88, 2019.
- [44] C. Savorgnan, C. Romani, A. Kozma, and M. Diehl, "Multiple shooting for distributed systems with applications in hydro electricity production," *J Process Control*, vol. 21, no. 5, pp. 738–745, 2011.
- [45] A. Mills, A. Wills, and B. Ninness, "Nonlinear model predictive control of an inverted pendulum," in *Amer. Contr. Conf.*, 2009, pp. 2335–2340.
- [46] J. B. Rawlings, D. Q. Mayne, and M. Diehl, *Model Predictive Control: Theory, Computation, and Design*. Nob Hill Publishing, 2019.
- [47] J. A. E. Andersson, J. Gillis, G. Horn, J. B. Rawlings, and M. Diehl, "CasADi: A software framework for nonlinear optimization and optimal control," *Math. Program. Comput.*, vol. 11, no. 1, pp. 1–36, 2019.
- [48] B. Stellato, G. Banjac, P. Goulart, A. Bemporad, and S. Boyd, "OSQP: An operator splitting solver for quadratic programs," *Math. Program. Comput.*, 2020.
- [49] A. Wächter and L. T. Biegler, "On the implementation of an interior-point filter line-search algorithm for large-scale nonlinear programming," *Math. Program.*, vol. 106, no. 1, pp. 25–57, 2006.
- [50] R. Findeisen, *Nonlinear Model Predictive Control: A Sampled-data Feedback Perspective*. VDI-Verlag, 2006.